1970

Turbulent structure in the wake of sphere

Darrell W. Pepper

Department:

TURBULENT STRUCTURE IN THE WAKE OF A SPHERE

BY

DARRELL WELDON PEPPER, 1946-

A THESIS

Presented to the Faculty of the Graduate School of the

UNIVERSITY OF MISSOURI-ROLLA

In Partial Fulfillment of the Requirements for the Degree

MASTER OF SCIENCE IN AEROSPACE ENGINEERING

1970

Approved by

S. C. Lee (Advisor) R B Duffey

David H. Montgomery

ABSTRACT

The study of turbulent wakes is considered necessary to understand the droplet behavior associated with the collision coalescence phenomena in atmospheric clouds. The Vertical Atmospheric Wind Tunnel enables experiments dealing with this droplet behavior to be analyzed.

The experiments conducted in the UMR Vertical Atmospheric Wind Tunnel consist of two parts: one is the investigation of the flow field characteristics in the test section of the wind tunnel; the other is the measurement of the turbulent structure in the wake of a sphere.

The test section is rectangular in design and has a cross-sectional area of 36 square inches (6 inches X 6 inches). Mean velocity profiles show the flow to be uniform but increasing in magnitude throughout the downstream portion of the test section. Boundary layer thickness becomes noticeable during the latter portion of the test section. Turbulence intensity, measured in the longitudinal direction of the test section at 10 different downstream positions by a DISA 55D01 hot-wire anemometer, show the background turbulence generated by the wind tunnel to be very small.

Mean velocity profiles in the wake of a sphere indicate rapid wake dissipation and show wake interaction with the wall boundary layer of the test section. Axisymmetric turbulence intensities are measured using an X-probe and two DISA 55D01 CTA units in both the Near and Far wakes of the sphere.

Reynolds shear stresses are likewise measured and the wake development analyzed through the turbulent energy equation.

ACKNOWLEDGMENT

The author wishes to express his sincerest gratitude to his advisor, Dr. Shen C. Lee, for his efforts in guiding this thesis. His invaluable assistance and help are largely responsible for the preparation of this thesis.

The author is grateful for the assistance given to him by Dr. R. B. Oetting, J. Auiler, and L. V. Field. Gratitude is also extended to the Department of Cloud Physics and Dr. J. L. Kassner, Jr. This project was supported in part under Themis grant N00014-68-A-0497 (2357-2228).

TABLE OF CONTENTS

LIST OF ILLUSTRATIONS

Page

Figures

Page

LIST OF TABLES

I. INTRODUCTION

Understanding the dynamics of water droplets for specific atmospheric conditions is very essential for meteorological applications. Measurements of droplet behavior within clouds have provided a great deal of information pertaining to this actual phenomena. However, the cause of this droplet behavior cannot be easily investigated because of the complex interactive problems which occur in nature. Consequently, in order to understand the flow characteristics associated with the drop under accurately controlled conditions, a vertical atmospheric wind tunnel for suspending droplets appears to be a desirable facility.

A prototype wind tunnel was first built at UCLA for cloud physics research within the Department of Meteorology. The UCLA tunnel is made of aluminum and stainless steel and incorporates a horizontal air conditioning unit and a vertical flow control system. Air speed can be controlled between 1 cm/sec and 8 m/sec in the observation section. The turbulence level is minimized by using a sonic nozzle between a 150 hp vacuum pump and the test section. Pruppacher and Beard (1) show velocity profiles to be very uniform and have successfully suspended droplets ranging in size from 10 to 450 microns under all temperature and humidity conditions.

INCA Engineering Company, builder of the UCLA cloud tunnel, built two additional wind tunnels based on the UCLA design. One was built for the National Center for Atmospheric Research at Boulder, Colorado, and the other for the UMR

Cloud Physics Research Center. Due to the limitations of the electric power supply, the UMR tunnel uses a series of five 1/4 hp centrifugal fans to provide the desired air velocity for suspending the droplets and incorporates a series of stilling chambers to minimize the turbulence. The air handling system of the UMR wind tunnel can be found in the thesis by Field (2).

Turbulence is a very important parameter when dealing with fluid motion. Because of the random variation of flow associated with turbulent motion, droplet behavior may become irregular. In order to examine the effect of the flow field characteristics of the free stream air on the droplet, the turbulence generated within the vertical atmospheric wind tunnel, known as background turbulence, must be investigated. Likewise, analyzing the turbulence produced within the UMR wind tunnel as compared with the UCLA tunnel will ascertain the validity of using five 1/4 hp centrifugal fans versus a 150 hp vacuum pump.

In order to study the dynamic behavior of rain drops, wherein droplets are assumed to spherical, one must understand the flow charateristics associated with the droplet. Specifically, the collision coalescence between water droplets has been observed to be strongly affected by the turbulent wake of a falling droplet (3). As a result, it is essential that turbulence studies be conducted in the wake of a sphere.

The study of turbulence behind a streamlined body is a classical subject. Townsend (4) has contributed much to the

analysis of two dimensional flow and has measured turbulence intensities as well as energy terms in the wake of a cylinder. Hinze (5) gives detailed accounts of experiments in two-dimensional wake flow and theoretically analyzes axisymmetric wake flow. Although much has been done in dealing with flows along solid boundaries, jets, and two dimensional wakes, very little has been done in experimentally analyzing axisymmetric turbulent wakes. Sami (6) has measured both turbulence intensity and turbulent energy diffusion terms (one point triple velocity correlations) in the wake of an air jet, and has contributed greatly to techniques of measuring various turbulence values for axisymmetric flow with hot-wire anemometry. Naudascher (7) has conducted experiments concerning the wake flow behind a self-propelled body and has measured mean-flow velocity and pressure, turbulence intensities in three directions, turbulent shear, auto-correlations of the axial velocity fluctuations behind a disk, and has analyzed free turbulence shear flow in detail. Chevray (8) has studied the turbulence behind a streamlined body of revolution including measurements of turbulence intensities in the longitudinal, axial, and radial directions and the mean cross products of turbulence in a radial plane throughout the flow, and presently is the only known work appearing in the literature. To the best knowledge of this author, no turbulence data on the wake of a sphere has yet appeared in any publication.

Investigation of the turbulence structure in the wake of a sphere would enable flow characteristics associated with a

droplet to be qualitatively understood and would contribute to an understanding of the rates of growth of the cloud drops to the size of precepitation particles by the collision-coalescence process.

II. EXPERIMENTAL EQUIPMENT

The experimental equipment consists of the vertical atmospheric wind tunnel, a spherical test model, and a series of instruments for pressure, velocity, and turbulent stress measurements.

A. Vertical Atmospheric Wind Tunnel

The vertical atmospheric wind tunnel, shown in Figure 1, is housed in the basement and first floor of the Cloud Physics Research Center. Air from the basement is pulled through the tunnel into a plenum, or settling chamber, from the downstream end of the system by a series of 1/4 hp centrifugal fans and rises upward through a series of honeycomb screens to the test section.

The test cross-section is 6 inches by 6 inches, has a length of 48 inches, and consists of rectangular plates of 1/2 inch thick plexiglass. Two of the plates may be removed in either the upper or lower section and replaced with instrumentation plates or glass plates for photographic purposes.

A diffusing section immediately follows the test section and tapers to provide area increase. Above the diffuser is a settling chamber which connects to ducting that returns to the basement. The ducting in the basement is connected to a settling chamber which contains the velocity control system, or pintle, as shown in Figure 2.

One end of the pintle is connected to the downstream ducting and draws air through the tunnel. The other end draws air through the inlet from the room. A settling chamber con-

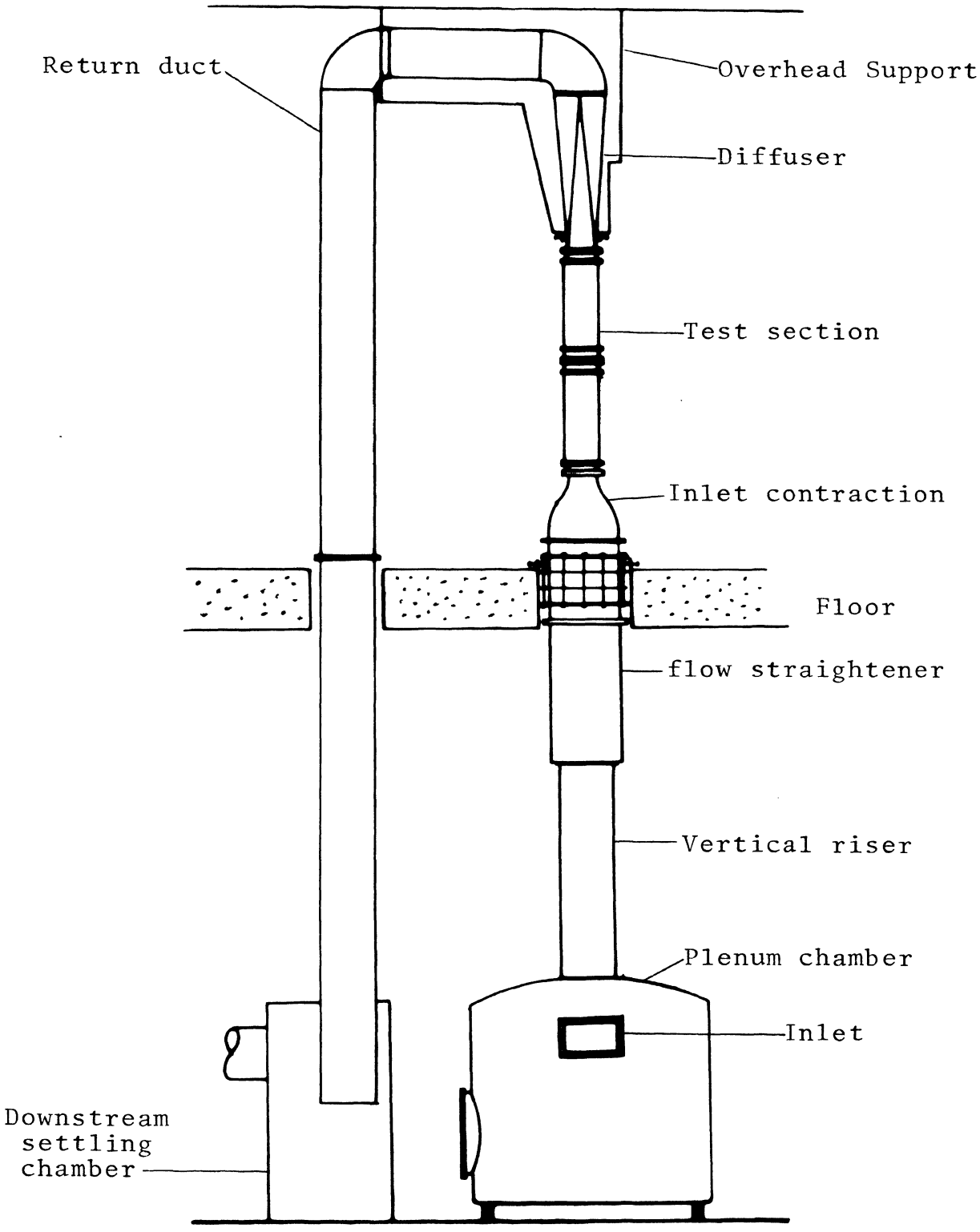

Figure 1. Vertical Atmospheric Wind Tunnel

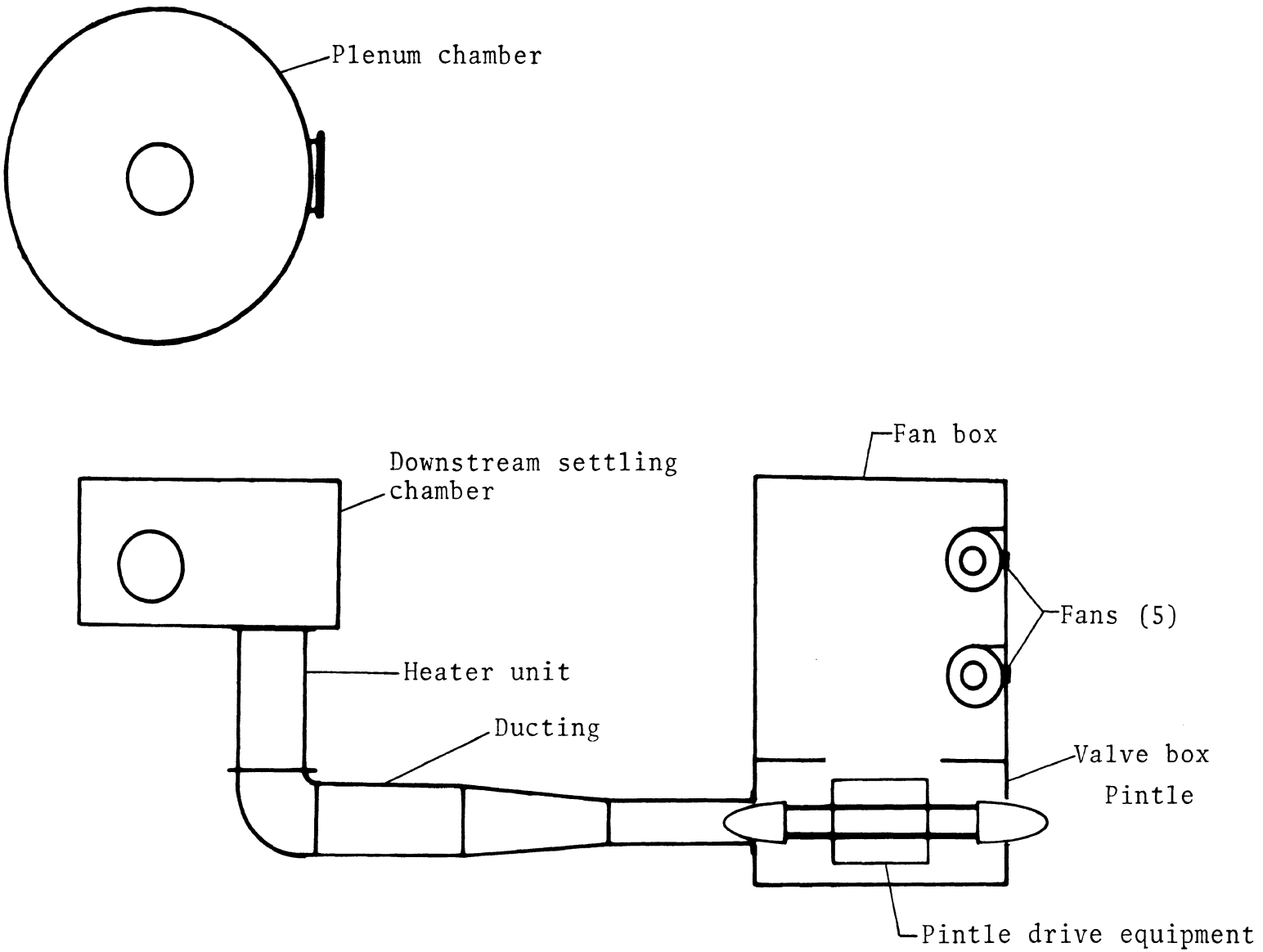

Figure 2. Velocity Control Equipment

nects to the pintle system and houses five 1/4 hp centrifugal fans. The five fans shown in Figure 2 are mounted to discharge directly to the surrounding atmosphere.

The control panel, which contains the fan switches and pintle displacement switch, is housed next to the test section on the first floor. A guage calibrated in pintle position is used to control the velocity from 1 cm/sec to 12 m/sec within the test section.

The air prehandling unit, consisting of a precooler, drying section, and humidifier system, was not connected because of a lack of an adequate cooling water supply for the refrigeration system. Consequently the air was neither humidified nor heated prior to entering the tunnel.

A complete description of the vertical atmospheric wind tunnel can be found in the thesis by Field (2).

B. Test Model (Sphere)

Experimental investigations in the wake of a falling water droplet have proven to be a most difficult task. Primarily two major problems are readily evident. First of all, the stability of the suspended droplet cannot be maintained if an instrument is physically placed in the wake. Secondly, the size of the falling droplet is comparatively too small for any reliable instrument to provide meaningful measurements of turbulence characteristics. Consequently, the wake structure of a large solid sphere may provide the necessary information for studying the wake capture phenomena associated with droplet collision coalescence.

A model of a sphere 1.25 inches in diameter was made and

placed in the tunnel, shown in Figure 3. The sphere, made of plexiglass, was mounted on a brass rod and supported by a tripod which rested on a honeycomb screen in the contraction section of the tunnel. The ratio of the cross-sectional area of the sphere to that of the test section was 1:13.5.

With the rod projecting into the stagnation side of the sphere, i.e., upstream of the sphere, the entire wake region of the sphere was clear of any support or obstacle which might hinder measurements. As the flow rate increased however, the spherical model began to oscillate significantly. Vibration was overcome by attaching wires to the rod just below the stagnation point. The interference between the wake of the wires and the wake of the sphere was minimized by using wire of 24 guage inclined approximately 70° to the brass rod. A picture of the test model and support system is shown in Figure 4.

C. Instrumentation

The equations of motion of turbulent flow consist of pressure, mean velocity, and fluctuating velocity terms. Hence, in order to study the dynamics associated with turbulent wakes behind a sphere, measurements of pressure, mean velocity, and fluctuating velocity are obtained through the following instrumentation:

1. Pressure Measurement Instrumentation

Pressure is measured by means of a pitot-static probe with its axis along the direction of flow and the total tap facing upstream. Using Bernoulli's Principle, the difference between total pressure and static pressure, ΔP, can be re-

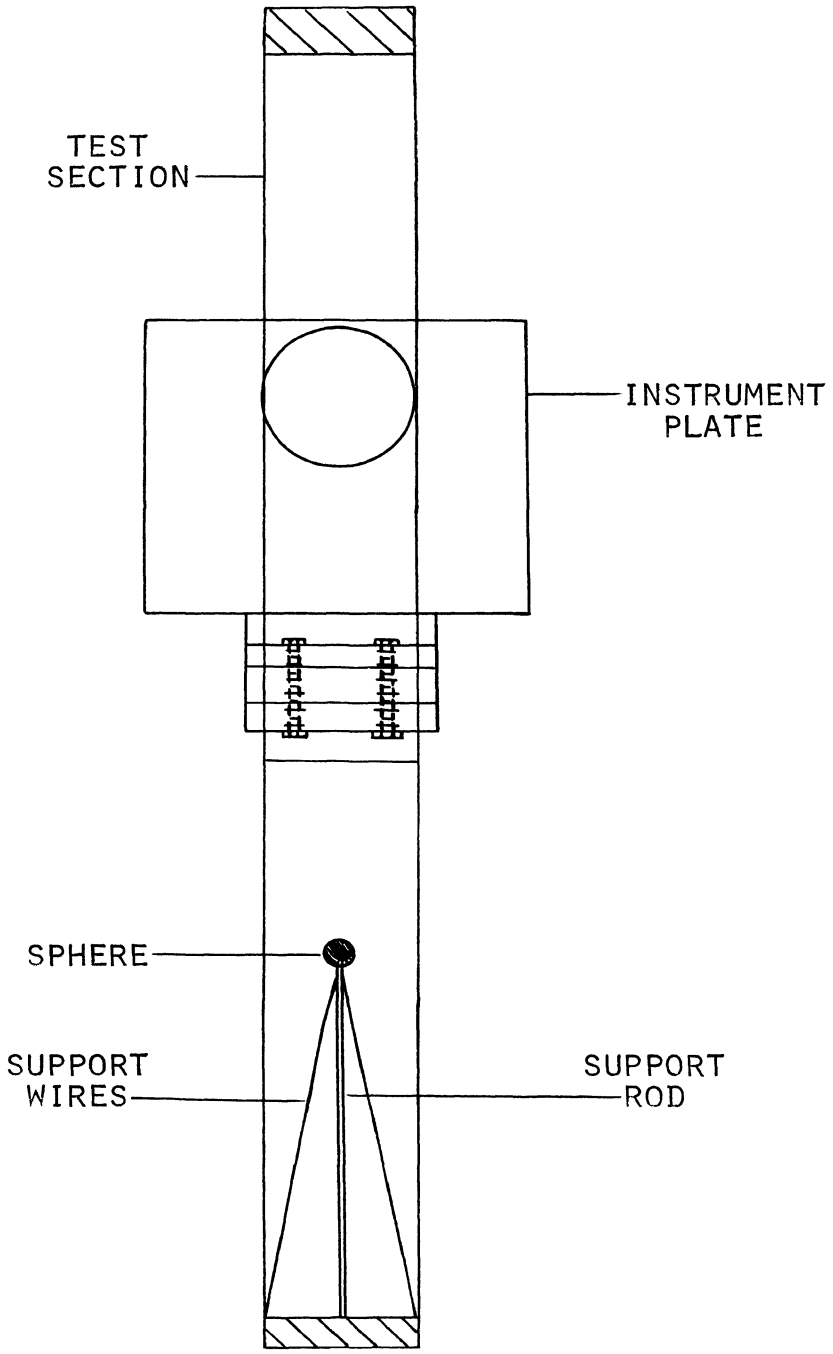

Figure 3. Test Section with Model Sphere

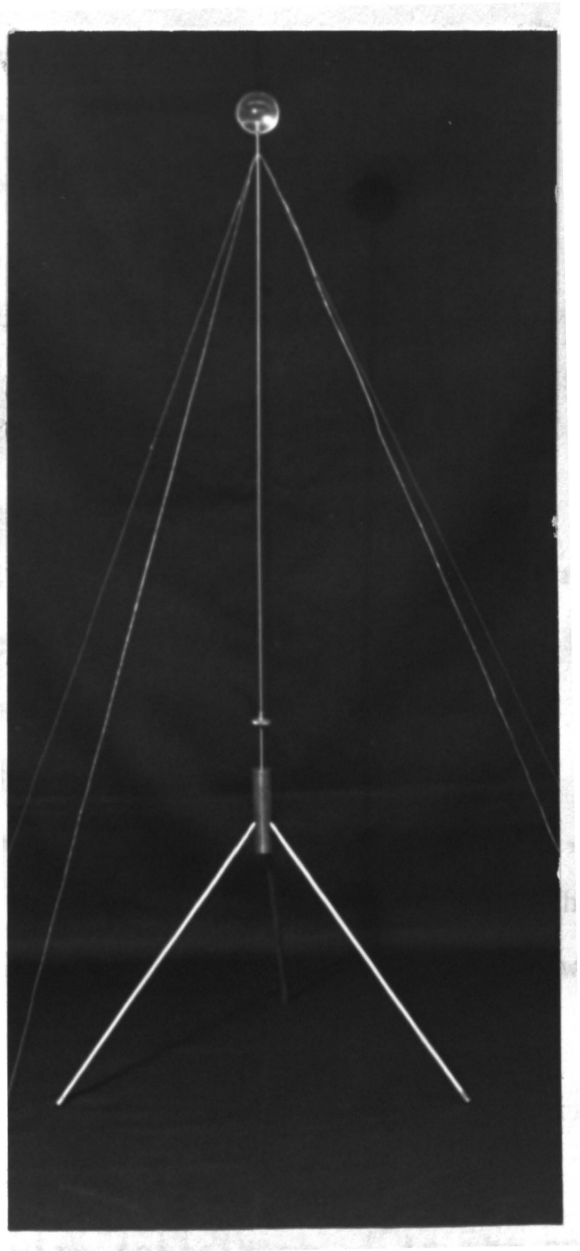

Figure 4. Model Sphere with Support

lated to a mean velocity through the equation

$$\Delta P = \frac{U^2 \rho}{2}$$

where ρ is the density of air and U is the mean velocity.

An MKS Baratron Electronic Pressure Meter, which allowed pressures in the range of 10^{-5} to 1000 mm Hg to be measured, was connected to the pitot-static probe and the mean velocity of the flow calculated by the equation above. Figure 5 shows the MKS meter attached to the wind tunnel control panel and the pitot-static probe. Pressure is read directly from the guage incorporated within the MKS meter.

2. Hot-wire Anemometer

Mean velocity and turbulent fluctuations can be measured by means of a hot-wire anemometer, either of the constant current type or the constant temperature type. A schematic diagram of both types is shown in Figure 6.

Both systems are based upon King's Law, which relates the balance between the energy due to electric heating and the energy due to convective cooling. King's Law, as described by Hinze (5), may be written as

$$\frac{I^2 R_w}{R_w - R_g} = A + BU^{.5} \qquad (2\text{-}1)$$

where R_w is the wire resistance, I is the current, R_g is the gas resistance, and A and B are constants determined by calibration techniques.

Equation (2-1) may also be written as

$$V^2 = V_o^2 + BU^{.5} \qquad (2\text{-}2)$$

where V is the voltage at a particular velocity, V_o is the

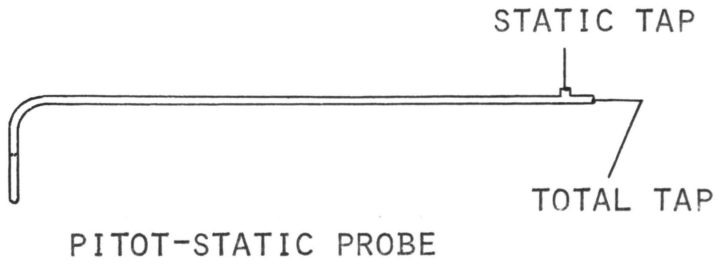

Figure 5. Velocity Control Panel and Pitot-Static Probe Instrumentation

Probec

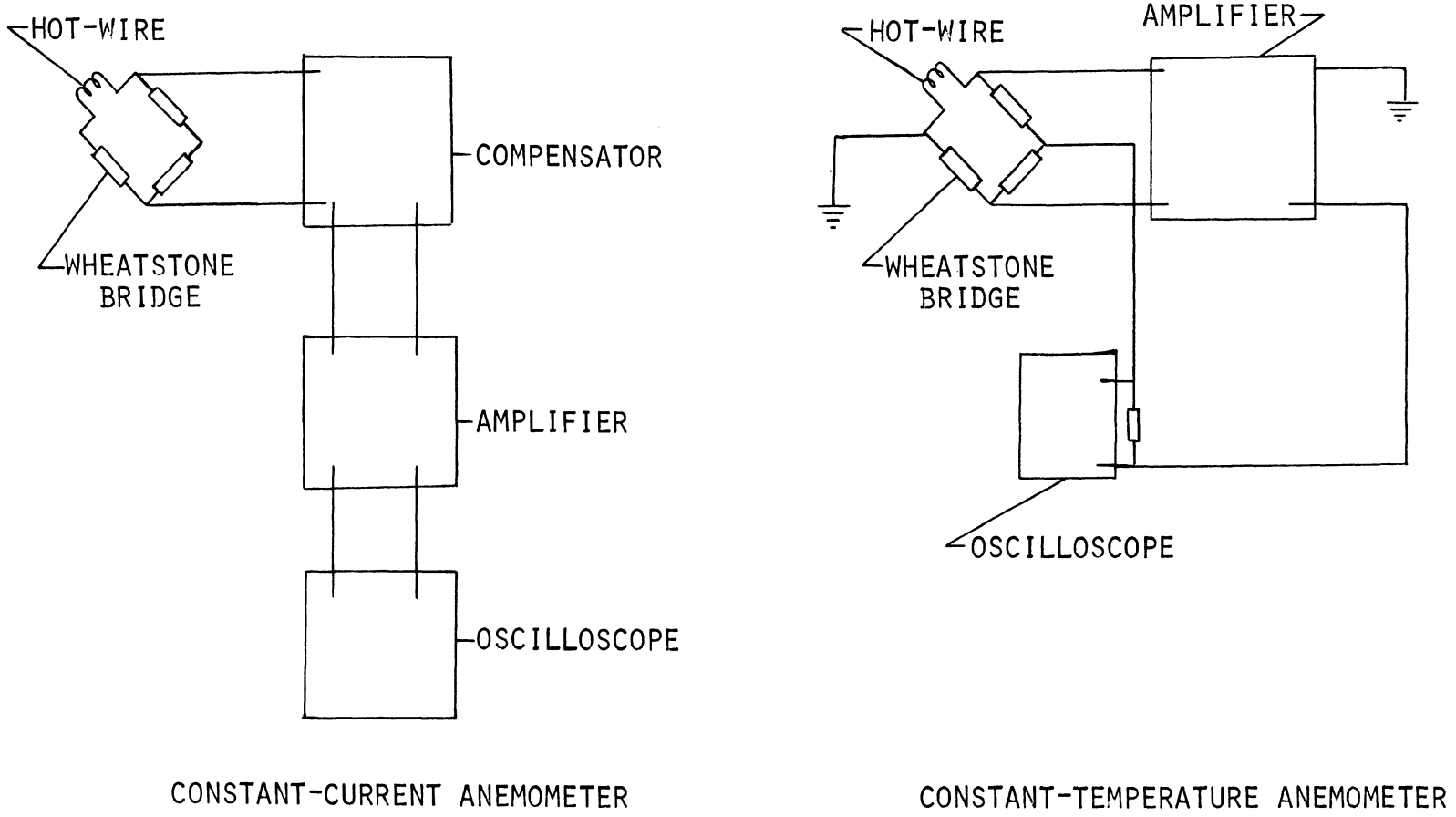

Figure 6. Hot-wire Anemometry Systems - Schematics

voltage at zero velocity, and B is a constant.

Fundamentally, the constant temperature anemometer consists of three basic elements: a wheatstone bridge, a servo-amplifier, and a sensing element.

The bridge is exactly balanced at a certain bridge voltage supplied by the servo-amplifier. A change in the probe resistance due to cooling results in an increase in the amplifier output current. The bridge voltage is adjusted so that the bridge is balanced whereby the amount of power supplied to keep the wire at constant temperature becomes directly proportional to the velocity of the medium.

The probe is a direction sensitive element consisting of a thin wire 5 microns in diameter suspended between two prongs. Mean velocity of a steady flow is determined by mounting the probe perpendicular to the direction of flow and measuring the DC voltage output signal from the wire. Calibration of the output signal with velocity recorded by the pitot-static probe gives the mean velocity of the flow.

Figures 7 and 8 show the single-wire and X-wire probes respectively with the hot-wire anemometry instrumentation. Figure 9 shows the single wire probe at 11 inches downstream of the inlet to the test section orientated to measure the lonitudinal turbulence intensity and mean velocity of the flow.

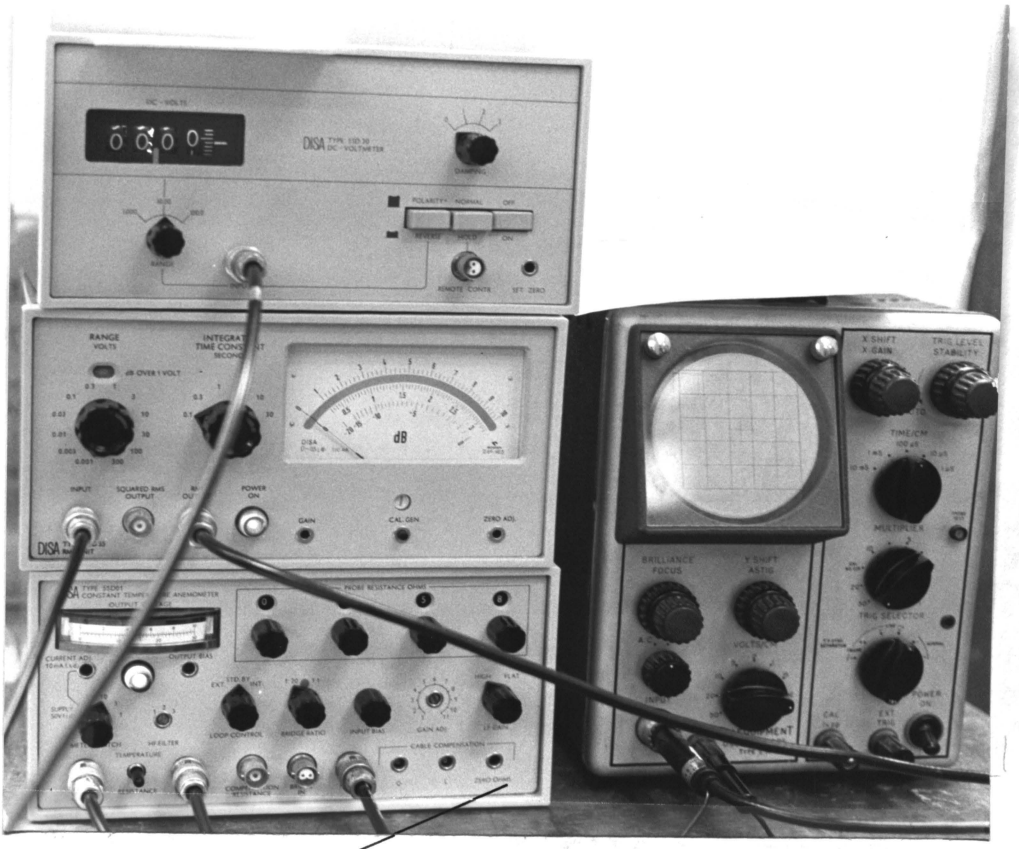

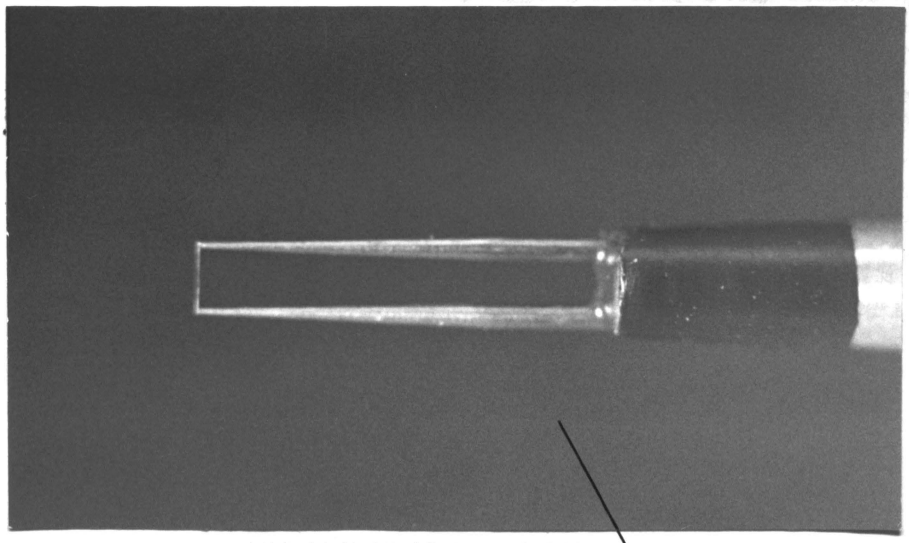

Figure 7. Single-wire Probe with Instrumentation

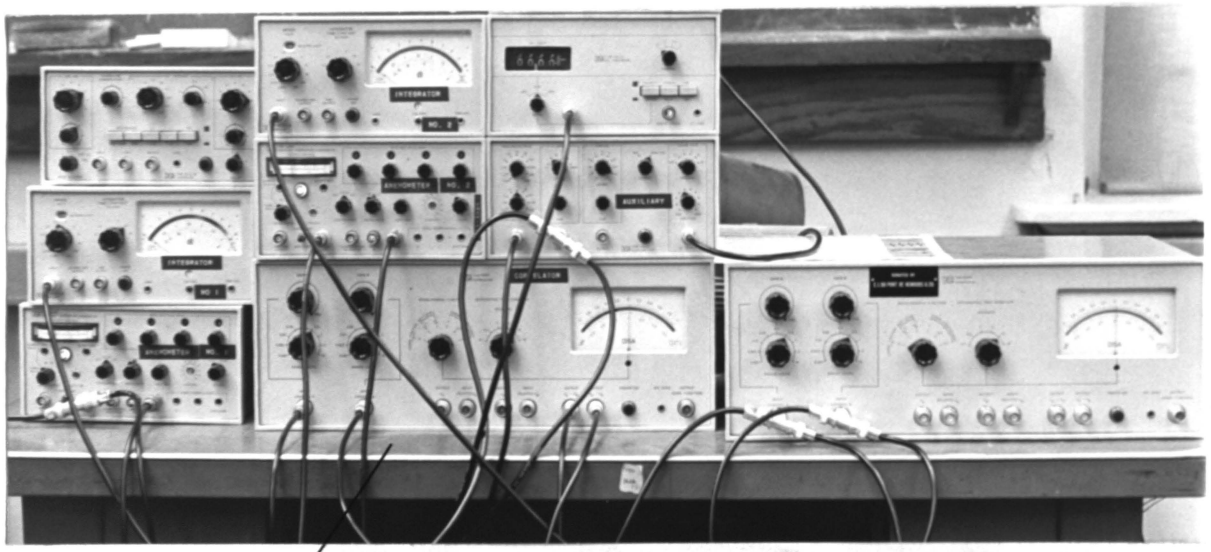

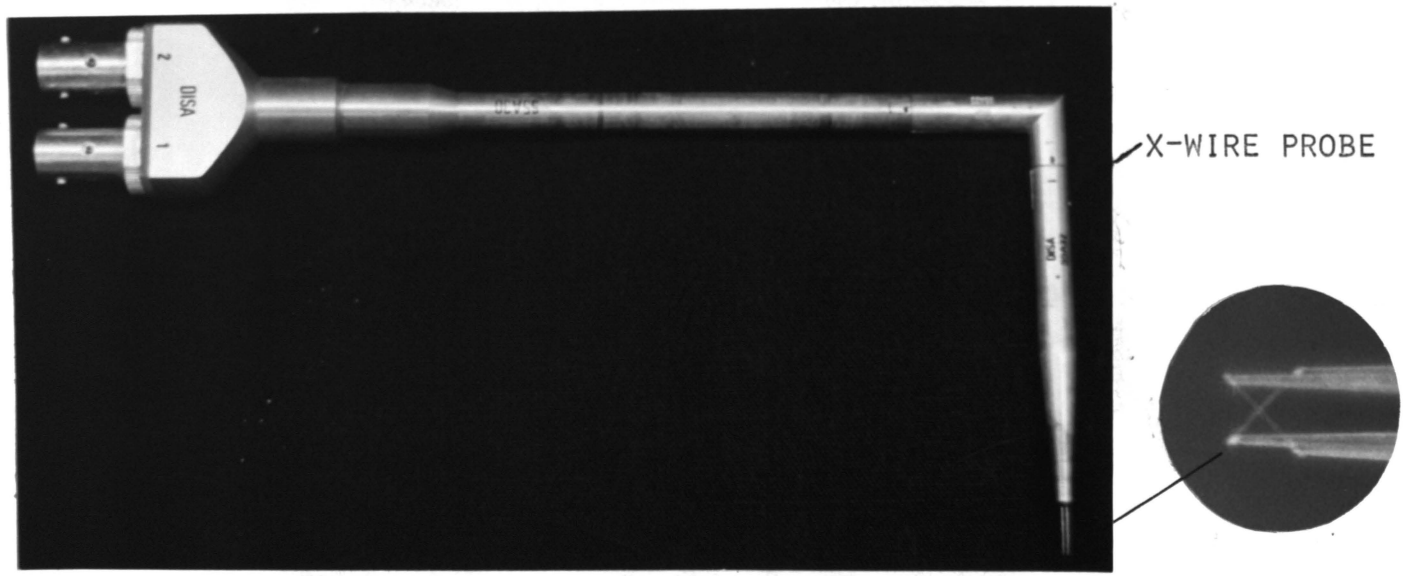

Figure 8. X-wire Probe with Instrumentation

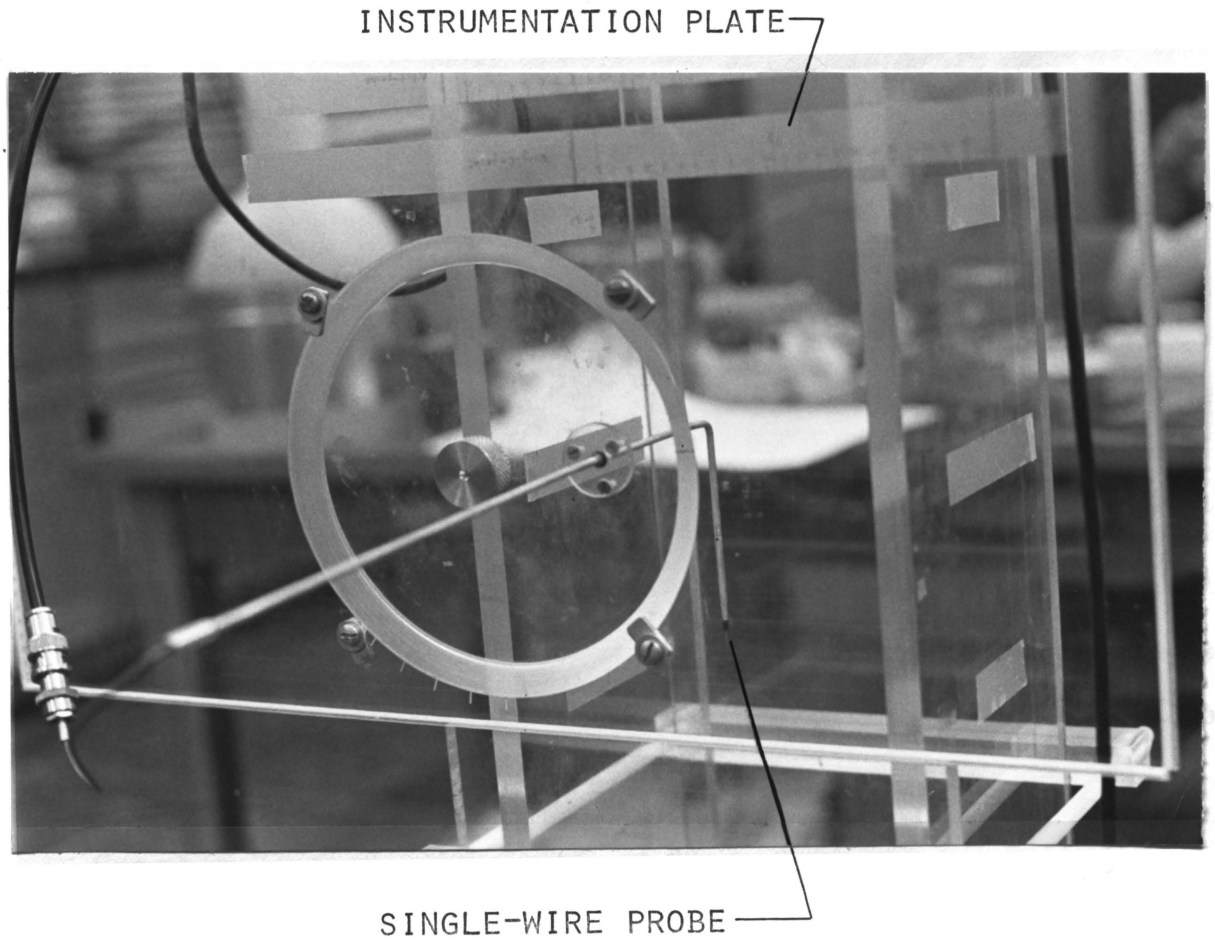

Figure 9. Single-wire Probe at z = 11 inches

III. TURBULENT STRUCTURE

It is fundamentally important that the significance of all flow parameters be analyzed qualitatively before any measurement is conducted. Since turbulence is composed of many minute fluctuations, it is necessary to consider the effect of these turbulence fluctuations on the equations of motion and on the special case of the experiment to be conducted.

A. General Equations of Motion

For velocities in the range of 1 to 10 m/sec in a quasi-steady state, the fluid can be considered to be incompressible.

Conservation of Mass may be written an

$$\frac{\partial}{\partial X_i} U_i = 0 \qquad (3\text{-}1)$$

where U_i is the velocity tensor in the X_i direction. The index i denotes the three spatial directions. The use of double indicies follows Einstein's summation convention as described by Hinze (5).

Conservation of Momentum is expressed by

$$\rho U_j \frac{\partial U_i}{\partial X_j} = F_i - \frac{\partial P}{\partial X_i} + \mu \frac{\partial^2 U_i}{\partial X_j \partial X_j} + \frac{\partial^2 U_j}{\partial X_i \partial X_j} \qquad (3\text{-}2)$$

where ρ is the density, F is the external forces, P is the pressure, and μ is the dynamic viscosity which is constant for a fluid a constant temperature.

B. General Turbulence Equations

Analysis of turbulence is based upon the assumption that the velocity at any instant can be expressed by

$$U_i = \overline{U_i} + u_i$$

where $\overline{U_i}$ is the time average velocity and u_i is the fluctuating velocity. Pressure and density are likewise represented in a similar relationship:

$$P = \overline{P} + p$$

$$\rho = \overline{\rho} + \rho'$$

Introducing these terms into the general equations of motion and time averaging, the conservation of mass takes the form

$$\frac{\partial}{\partial X_i}\overline{U_i} = 0 \tag{3-3}$$

while the momentum equation becomes

$$\overline{\rho}\,\overline{U_j}\frac{\partial \overline{U_i}}{\partial X_j} = \overline{F_i} - \frac{\partial \overline{P}}{\partial X_i} + \frac{\partial}{\partial X_j}\left(\mu\frac{\partial \overline{U_i}}{\partial X_j} - \overline{\rho u_i u_j}\right) \tag{3-4}$$

where the term $\overline{\rho u_i u_j}$ is the Reynolds shear stress.

The occurrence of the Reynolds shear stress causes a major problem when solving turbulent flow problems. Empirical expressions of these shear stresses have been postulated from phenomenological theories which can be found in Hinze (5) and Schlichting (9).

The actual turbulence behavior of a fluid, however, can only be studied through the turbulence energy, since it is of a dissipative and productive nature. The turbulent energy equation is written as

$$\underset{(I)}{\frac{d}{dt}\frac{\overline{q^2}}{2}} = \underbrace{-\frac{\partial}{\partial X_i}\overline{u_i\left(\frac{P}{\rho} + \frac{q^2}{2}\right)}}_{(II)} - \underbrace{\overline{u_i u_j}\frac{\partial \overline{U_j}}{\partial X_i}}_{(III)} + \underbrace{\frac{1}{2}\left(\nu\frac{\partial^2 \overline{q}}{\partial X_i \partial X_i}\right)}_{(IV)} - \underbrace{\nu\overline{\frac{\partial u_j}{\partial X_i}\frac{\partial u_j}{\partial X_i}}}_{(V)} \tag{3-5}$$

where q is the turbulent kinetic energy and is defined as $q^2 = u_i u_i$ and ν is the kinematic viscosity. Term I is the change in kinetic energy of turbulence, term II is the convective diffusion by turbulence, term III is the production of turbulence energy, term IV is the work done by the viscous shear stresses, and term V is the dissipation of turbulent motion.

In order to study the physical meaning of each term when conducting an experimental analysis in the wake of a sphere, the governing equations need to be expressed in an axisymmetric coordinate system.

C. Axisymmetric Turbulence Equations

The governing equations for axisymmetric flow are described in terms of cylindrical coordinates where U_r, U_θ, and U_z refer to the direction of r, θ, and z respectively, as seen in Figure 10. Assuming rotational symmetry, the conservation of mass is written as

$$\frac{1}{r}\frac{\partial}{\partial r}(rU_r) + \frac{\partial}{\partial z}(U_z) = 0 \qquad (3\text{-}6)$$

where U_r is the mean radial velocity and U_z is the longitudinal mean velocity.

The momentum equation is written in cylindrical coordinates for the radial component as

$$\rho\left(U_r\frac{\partial U_r}{\partial r} - \frac{U_\theta^2}{r} + U_z\frac{\partial U_r}{\partial z}\right) = \rho g_r - \frac{\partial P}{\partial r} + \mu\left[\frac{\partial}{\partial r}\left(\frac{1}{r}\frac{\partial}{\partial r}(rU_r)\right) + \frac{\partial^2 U_r}{\partial z^2}\right] \qquad (3\text{-}7)$$

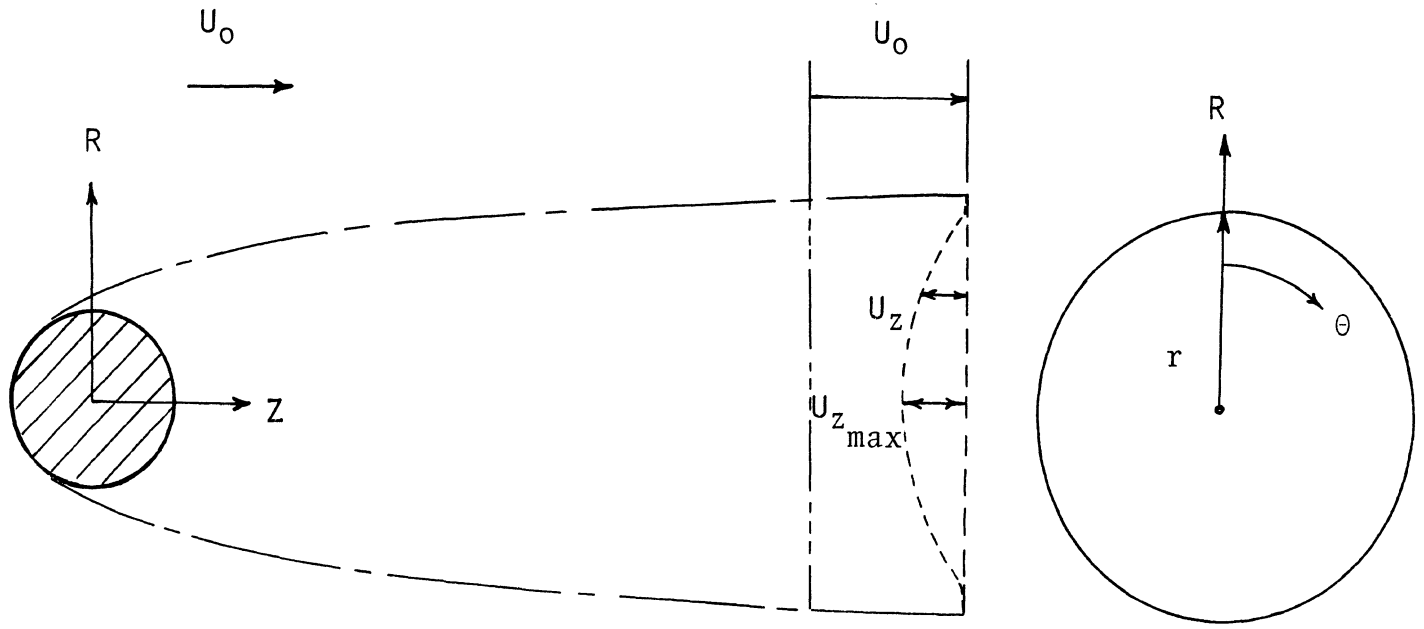

Figure 10. Scheme of Wake Flow Behind a Sphere

where U_θ is the axial mean velocity, ρ is the density, and F_r is the radial body force.

Introducing the concept of a mean value plus a fluctuating value for velocity, density, and pressure terms and time averaging, the equations of motion for axisymmetric flow take the form

r-direction:

$$\bar{\rho}\left(\overline{U_r}\frac{\partial \overline{U_r}}{\partial r} + \overline{U_z}\frac{\partial \overline{U_r}}{\partial z} - \frac{\overline{U_\theta^2}}{r}\right) = -\frac{\partial \bar{P}}{\partial r} + \mu\left(\nabla^2 \overline{U_r} - \frac{\overline{U_r}}{r^2}\right)$$
$$- \frac{\bar{\rho}}{r}\frac{\partial}{\partial r} r\overline{u_r^2} - \bar{\rho}\frac{\partial}{\partial z}\overline{u_r u_z} + \bar{\rho}\frac{\overline{u_\theta^2}}{r} + \bar{F}_r \qquad (3\text{-}8)$$

θ-direction:

$$\bar{\rho}\left(\overline{U_r}\frac{\partial \overline{U_\theta}}{\partial r} + \overline{U_z}\frac{\partial \overline{U_\theta}}{\partial z} + \frac{\overline{U_r U_\theta}}{r}\right) = \mu\left(\nabla^2 \overline{U_\theta} - \frac{\overline{U_\theta}}{r^2}\right) - \bar{\rho}\frac{\partial}{\partial r}\overline{u_\theta u_r}$$
$$- \bar{\rho}\frac{\partial}{\partial z}\overline{u_\theta u_z} - 2\bar{\rho}\frac{\overline{u_\theta u_r}}{r} + \bar{F}_\theta \qquad (3\text{-}9)$$

z-direction:

$$\bar{\rho}\left(\overline{U_r}\frac{\partial \overline{U_r}}{\partial r} + \overline{U_z}\frac{\partial \overline{U_z}}{\partial z}\right) = -\frac{\partial \bar{P}}{\partial z} + \mu\nabla^2 \overline{U_z} - \bar{\rho}\frac{\partial}{\partial z}\overline{u_z^2} + \bar{F}_z$$
$$- \frac{\bar{\rho}}{r}\frac{\partial}{\partial r} r\overline{u_r u_z} \qquad (3\text{-}10)$$

where ∇^2 is defined as a vector operator in cylindrical coordinates and $\bar{F}$ is the external body force.

The energy equation is derived for an incompressible, axially-symmetric, steady flow by Naudascher (7) and Sami (6) in explicit detail. Primarily, the procedure consists of

multiplying each of the equations of motion by its corresponding component of velocity and averaging with respect to time after the multiplication, then adding the terms together. After this has been done, the Reynolds equations are multiplied by their corresponding components of mean velocity and the terms added together. By substracting this last equation from the one previously formulated gives the turbulent energy equation. The turbulent energy equation, assuming no body forces and no axial components, is written as

$$- \bar{\rho}\left[\overline{u_z^2}\frac{\partial \bar{U}_z}{\partial z} + \overline{u_r^2}\frac{\partial \bar{U}_r}{\partial r} + \overline{u_r^2}\frac{\bar{U}_r}{r} + \overline{u_z u_r}\left(\frac{\partial \bar{U}_z}{\partial r} + \frac{\partial \bar{U}_r}{\partial z}\right)\right] - \left[\frac{\partial}{\partial z}\overline{u_z p}\right.$$

$$\left. + \frac{1}{r}\frac{\partial}{\partial r}(\overline{r u_r p})\right] + \frac{\mu}{r}\left\{ r\frac{\partial}{\partial z}\left[\frac{\partial}{\partial z}\left(\frac{\overline{q^2}}{2}\right) + \frac{\partial \overline{u_z^2}}{\partial z} + \frac{1}{r}\frac{\partial}{\partial r}(\overline{r u_z u_r})\right]\right.$$

$$\left. + \frac{\partial}{\partial r} r\left[\frac{\partial}{\partial r}\left(\frac{\overline{q^2}}{2}\right) + \frac{\partial(\overline{u_z u_r})}{\partial z} + \frac{1}{r}\frac{\partial}{\partial r}(\overline{r u_r^2}) - \frac{\overline{u_\theta^2}}{r}\right]\right\} = \frac{\bar{\rho}}{2}\left[\bar{U}_z\frac{\partial \overline{q^2}}{\partial z}\right.$$

$$\left. + \bar{U}_r\frac{\partial \overline{q^2}}{\partial r}\right] + \frac{\bar{\rho}}{2}\left[\frac{\partial}{\partial z}(\overline{u_z q^2}) + \frac{1}{r}\frac{\partial}{\partial r}(\overline{r u_r q^2})\right] + \Delta \qquad (3\text{-}11)$$

where the left hand side of the equation represents the rate at which work is done per unit volume while the right hand side determines the rate of energy change.

The term Δ is defined as

$$\Delta = \mu\left[2\left(\frac{\partial \bar{u}_z}{\partial z}\right)^2 + 2\left(\frac{\partial \bar{u}_r}{\partial r}\right)^2 + 2\left(\frac{\bar{u}_r}{r}\right)^2 + \left(\overline{\frac{\partial u_z}{\partial r} + \frac{\partial u_r}{\partial z}}\right)^2\right.$$

$$\left. + \left(\frac{\partial \bar{u}_\theta}{\partial z}\right)^2 + \left(\overline{\frac{\partial u_\theta}{\partial r} - \frac{u_\theta}{r}}\right)^2\right] \qquad (3\text{-}12)$$

where μ is the dynamic viscosity. If the Reynolds number is sufficiently high, the mean viscous stresses can be neglected. Assuming isotropic conditions, Δ becomes

$$\Delta \simeq 15\mu \left(\frac{\partial \overline{u}}{\partial z}\right)^2$$

This approximation is known as the Kolmogoroff approximation and is explained in detail by Naudascher (7).

Notice that the energy equation contains single, double, and triple velocity terms. These velocity terms, known as single, double, and triple correlations, can be measured using hot-wire anemometry and the turbulent behavior of the flow ascertained.

IV. HOT-WIRE ANEMOMETRY

Since the constant temperature anemometer measures flow parameters in terms of electrical responses, it becomes necessary to transform the turbulent terms to be measured into equations consisting of voltages and frequency responses. Consequently, a general understanding of King's Law and the velocity components associated with single and X-wire probes is needed. The equations and derivations which follow are derived primarily for use with a DISA 55D01 CTA and relate turbulence terms in meters per second to voltage fluctuations recorded by the CTA unit.

A. Basic Equations

The fundamental concepts of anemometry are essentially based on the formula postulated by King, given as

$$V^2 = V_o^2 + BU^{.5} \tag{4-1}$$

where V is defined as bridge voltage, V_o is the voltage output at zero flow velocity, B is a constant, and U is the mean velocity. Rearranging the equation above and solving for U gives the equation

$$U = (V^2 - V_o^2)^2 B^{-2} \tag{4-2}$$

Differentiation of equation (4-2) results in

$$dU = d\bar{U} + du$$

or

$$dU = du$$

Consequently,

$$du = 4\left[\frac{V}{(V^2 - V_o^2)}\right]\left[\frac{1}{(V^2 - V_o^2)}\right]^{-2}\left(\frac{dV}{B}\right)B^{-1}$$

Dividing both sides by U gives

$$\frac{du}{U} = \left[\frac{4V^2}{(V^2 - V_o^2)}\right]\frac{dV}{V} \qquad (4-3)$$

where du is the root mean square velocity and dV is the root mean square value of the bridge voltage. The longitudinal turbulence intensity can therefore be defined from this simple relation as

$$\frac{u'}{U} = \frac{4}{1 - \left(\frac{V_o}{V}\right)^2}\frac{\sqrt{e^2}}{V} \qquad (4-4)$$

where u' is defined as the root mean square of the the fluctuating velocity $\sqrt{u^2}$, $\sqrt{e^2}$ is equal to dV, and V is the output voltage from the anemometer.

Hinze (5) also defines a relation between u' and the corresponding root-mean-square (rms) voltage by introducing a sensitivity factor, given by

$$su' = \sqrt{e^2} \qquad (4-5)$$

where s is the sensitivity factor of a single wire.

If two hot-wires are placed in an X-array and displaced symmetrically about the mean flow direction, the wires will be equally excited by u but oppositely excited by v, as shown in Figure 11.

With the condition that the X-wires are mounted mutually 45^o to the direction of flow, the following equations are ob-

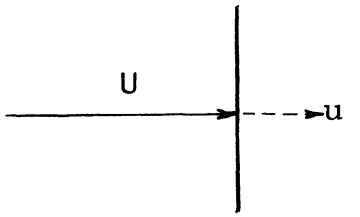

SINGLE-WIRE

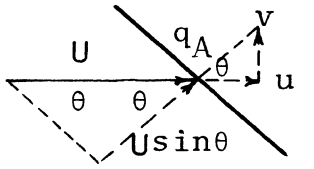

X-WIRE (A)

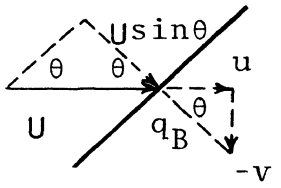

X-WIRE (B)

Figure 11. Measurement of Turbulent Velocities Using Single-wire and X-wire Probes

tained:

$$u\ (\sin\theta) + v\ (\cos\theta) = Q_A$$

$$u\ (\sin\theta) - v\ (\cos\theta) = Q_B$$

where Q_A and Q_B are defined as fluctuating velocities normal to wires A and B, respectively.

For $\theta = 45^o$, and solving for u' from the two above equations:

$$u' = \sqrt{\frac{1}{2}\left(\overline{q^2_{A_{xz}}} + \overline{q^2_{B_{xz}}}\right) + \overline{q_{A_{xz}} q_{B_{xz}}}} \qquad (4\text{-}6)$$

where q denotes the fluctuating velocity normal to the wire, and xz denotes the x-z planes the wire is orientated. v' is found by taking the difference between Q_A and Q_B such that v' becomes

$$v' = \sqrt{\frac{1}{2}\left(\overline{q^2_{A_{xz}}} + \overline{q^2_{B_{xz}}}\right) - \overline{q_{A_{xz}} q_{B_{xz}}}} \qquad (4\text{-}7)$$

Likewise, w' can be found by rotating the X-wire configuration into the y-z plane.

The cross-correlation coefficient is now introduced, given by the equation

$$\rho_{AB} = \frac{\overline{q_A q_A}}{\sqrt{\overline{q^2_A}}\sqrt{\overline{q^2_B}}} \qquad (4\text{-}8)$$

where ρ_{AB} is the cross-correlation coefficient, and q_A and q_B are still assumed to be orientated in the x-z plane.

To solve equation (4-6) for u', for example, use is made of the cross-correlation factor such that

$$\frac{\sqrt{\overline{q_{A_{xz}}^2}}}{U \sin\theta} = \frac{4}{1 - \left(\frac{V_o}{V}\right)^2} \frac{\sqrt{\overline{e_A^2}}}{V_A}$$

where U is the free stream velocity and $\theta = 45^o$. A similar expression is obtained for $\overline{q_{B_{xz}}^2}$. Substitution of $\overline{q_{A_{xz}}^2}$ and $\overline{q_{B_{xz}}^2}$ into equation (4-6) gives

$$u' = \left[\frac{1}{2} \left\{ \left[\frac{4U \sin\theta}{1 - \left(\frac{V_o}{V_A}\right)^2} \frac{1}{V_A} \right]^2 \overline{e_A^2} + \left[\frac{4U \sin\theta}{1 - \left(\frac{V_o}{V_B}\right)^2} \frac{1}{} \right]^2 \overline{e_B^2} \right\} \right.$$

$$\left. + \frac{\rho_{AB}}{V_A V_B} \left[\frac{4U \sin\theta}{1 - \left(\frac{V_o}{V_A}\right)^2} \right] \left[\frac{4U \sin\theta}{1 - \left(\frac{V_o}{V_B}\right)^2} \right] \right]^{\frac{1}{2}} \qquad (4\text{-}9)$$

Equations for v' and w' are derived in a similar manner.

Since the above quantities are difficult to measure and require a considerable amount of time to solve, an alternate method is used.

By equating the bridge voltages, i.e., $V_A = V_B$, the sensitivities should be equal for either wire. This procedure gives

$$e_A = s_1(u) + s_2(v)$$

$$e_B = s_1(u) - s_2(v)$$

Hence, letting $s_1 = s_2$,

$$e_A = s(u + v)$$

$$e_B = s(u - v) \qquad (4\text{-}10)$$

where $s = s_1 = s_2$.

The sum and difference of the voltage signals e_A and e_B result in

$$e_A + e_B = 2su$$
$$e_A - e_B = 2sv \qquad (4\text{-}11)$$

Taking the root-mean-square of both sides gives

$$u' = \frac{1}{2s}\sqrt{\overline{(e_A + e_B)^2}} \qquad (4\text{-}12)$$

and

$$v' = \frac{1}{2s}\sqrt{\overline{(e_A - e_B)^2}} \qquad (4\text{-}13)$$

In like manner, w' is written as

$$w' = \frac{1}{2s}\sqrt{\overline{(e_{A_{90^o}} - e_{B_{90^o}})^2}} \qquad (4\text{-}14)$$

where the 90^o denotes the X-wire being rotated 90^o about the z axis from the original configuration for measuring u' and v'. The sensitivity, s, is defined for u', v', and w' equations as

$$s = \left[1 - \left(\frac{V_o}{V}\right)^2\right]\frac{V}{4U} \qquad \text{(volts/m/sec)}$$

To find the longitudinal turbulence intensity $\left(\frac{u'}{U}\right)$, use is made of the equation

$$\frac{u'}{U \sin\theta} = \frac{1}{2s}\sqrt{\overline{(e_A + e_B)^2}}\ U^{-1}$$

which can also be written as

$$\frac{u'}{U} = \frac{.707}{2s}\sqrt{\overline{(e_A + e_B)^2}}\ U^{-1} \qquad (4\text{-}15)$$

where s, $\sqrt{\overline{(e_A + e_B)^2}}$, and $\sqrt{\overline{(e_A - e_B)^2}}$ are quantities measured by the hot-wire anemometer.

B. Reynolds Shear Stress

The Reynolds shear stresses, u'v' and u'w', are derived from the equations

$$\begin{aligned} \sqrt{2}\ q_{A_{xz}} &= u + v \\ \sqrt{2}\ q_{B_{xz}} &= u - v \end{aligned} \tag{4-16}$$

These equations can be easily obtained from equations (4-6) and (4-7).

If both equations of (4-16) are squared, then the difference taken, the result becomes

$$2uv = q_{A_{xz}}^2 - q_{B_{xz}}^2$$

or, taking the root-mean-square of both sides,

$$\sqrt{\overline{u^2}}\sqrt{\overline{v^2}} = \frac{1}{2}\sqrt{\overline{(q_{A_{xz}}^2 - q_{B_{xz}}^2)^2}}$$

which can also be written as

$$u'v' = \frac{1}{2}\sqrt{\overline{(q_{A_{xz}}^2 - q_{B_{xz}}^2)^2}} \tag{4-17}$$

Rotation of the X-wire into the y-z plane results in

$$u'w' = \frac{1}{2}\sqrt{\overline{(q_{A_{yz}}^2 - q_{B_{yz}}^2)^2}} \tag{4-18}$$

The Reynolds shear stresses can also be written in cylindrical coordinates as $u_z'u_r'$ and $u_z'u_\theta'$ where r denotes the radial direction and θ denotes the axial direction (u_z' corresponds to the u' in the longitudinal direction, i.e, the z direction as implied in equation (4-4)).

Equations (4-17) and (4-18) are general equations written for any coordinate system, although they imply a cartesian coordinate system. By letting u denote the longitudinal direction, v one of the lateral directions, and w the other lateral direction, a transformation from cartesian to cylindrical coordinates can readily be made. Hence,

$$u' \equiv u'_z \quad \text{(longitudinal)}$$
$$v' \equiv u'_r \quad \text{(radial)}$$
$$w' \equiv u'_\theta \quad \text{(axial)}$$

By making this assumption, the turbulence intensities as well as the Reynolds shear stresses derived in this chapter will apply to measurements in the wake of a sphere as well as to measurements in the test section (rectangular) of the wind tunnel.

To simplify matters, the cross-correlation factor R_{AB} is introduced. The sum and difference signals can be correlated in a manner similar to the method used for the cross-correlation coefficient such that R_{AB} becomes a direct function of the shear stress. R_{AB} is defined by

$$R'_{AB} = \overline{e_{sum} e_{difference}}$$

where $\overline{e_{sum}} = \sqrt{\overline{(e_A + e_B)^2}}$ and $\overline{e_{difference}} = \sqrt{\overline{(e_A - e_B)^2}}$.
This results in

$$R_{AB} = R'_{AB} G_A G_B$$

or,

$$R_{AB} = G_A G_B \overline{e_{sum} e_{difference}} \qquad (4\text{-}19)$$

where G_A and G_B are attenuator settings on the DISA 55D70 Correlator (see Appendix B for further details). However,

$$e_{sum} = 2su$$
$$e_{difference} = 2sv \qquad (4\text{-}20)$$

so that

$$4s^2\overline{u'v'} = G_A G_B \overline{e_{sum} e_{difference}}$$

or

$$\overline{u'v'} = \frac{R'_{AB}\, G_A\, G_B}{4s^2} \qquad (4\text{-}21)$$

V. RESULTS AND DISCUSSION

The experimental results on the turbulence characteristics are discussed in two parts: one is the flow field characteristics within the wind tunnel test section; the other is the turbulence structure in the wake of a sphere.

A. Flow Field Characteristics in the Test Section of the Vertical Atmospheric Wind Tunnel

Information of the flow field characteristics in the test section is necessary prior to the experimental investigation in the wake of a sphere. The average velocity, turbulence intensity, and the boundary layer thickness were measured for two different fan settings.

1. Average Tunnel Velocity

Ten separate locations were measured for each fan setting, ranging from 7 inches to 46 inches downstream of the inlet of the test section. Figures 12 and 13 show velocity distributions for both one and two fan configurations, respectively. Notice that the velocity distribution is fairly uniform at each cross-section. However, the average velocity increases slightly as the flow proceeds downstream. This is due to the boundary layer build-up along the walls of the test section. No measurements could be recorded between 19 inches and 28 inches because of a joint which connected the two plexiglass test sections together.

In order to maintain constant average velocity throughout the test section, it appears necessary to diverge the walls at a small angle to allow the boundary layer to build

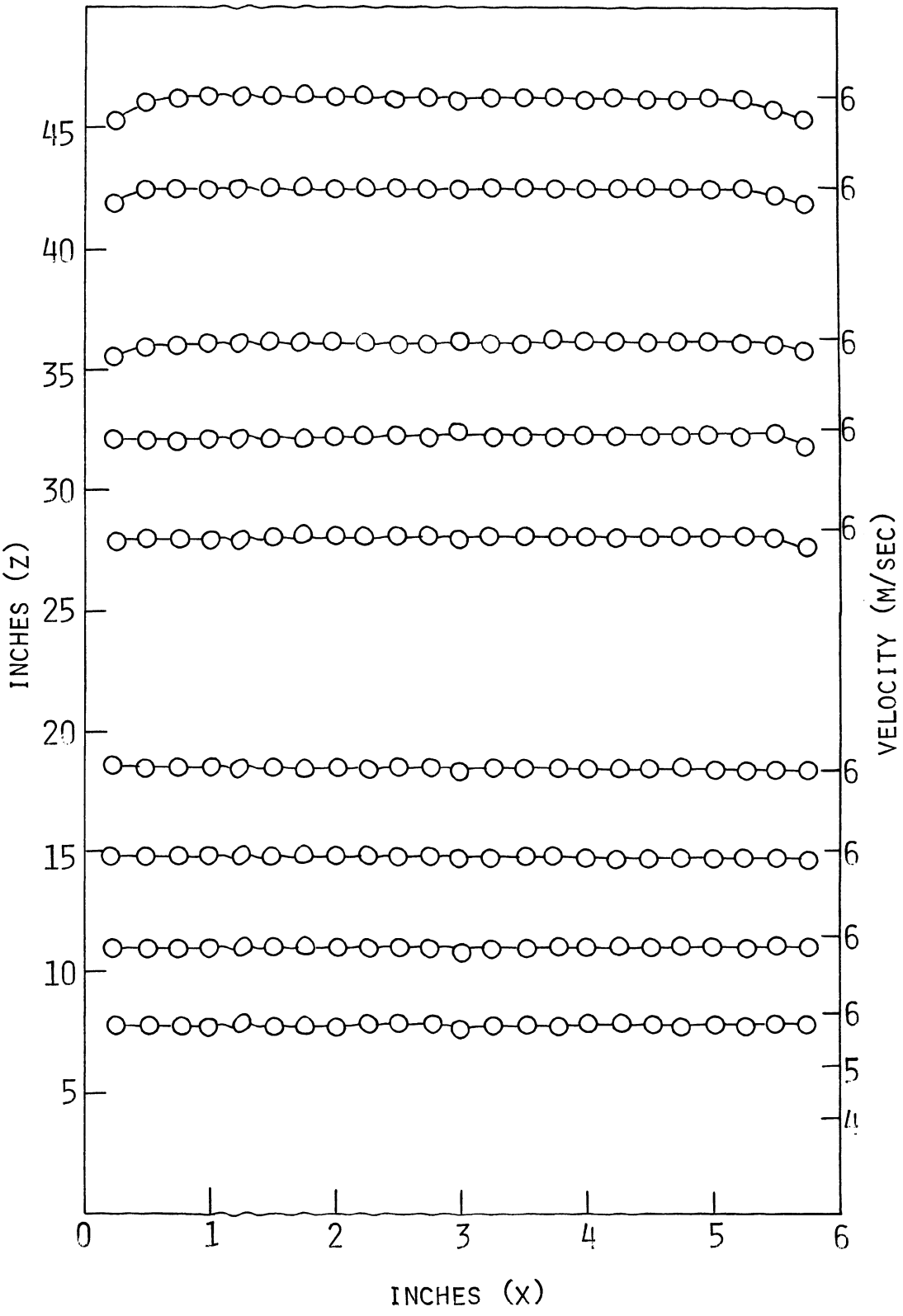

Figure 12. Mean Velocity Profile for U_o = 6.15 meters/sec.

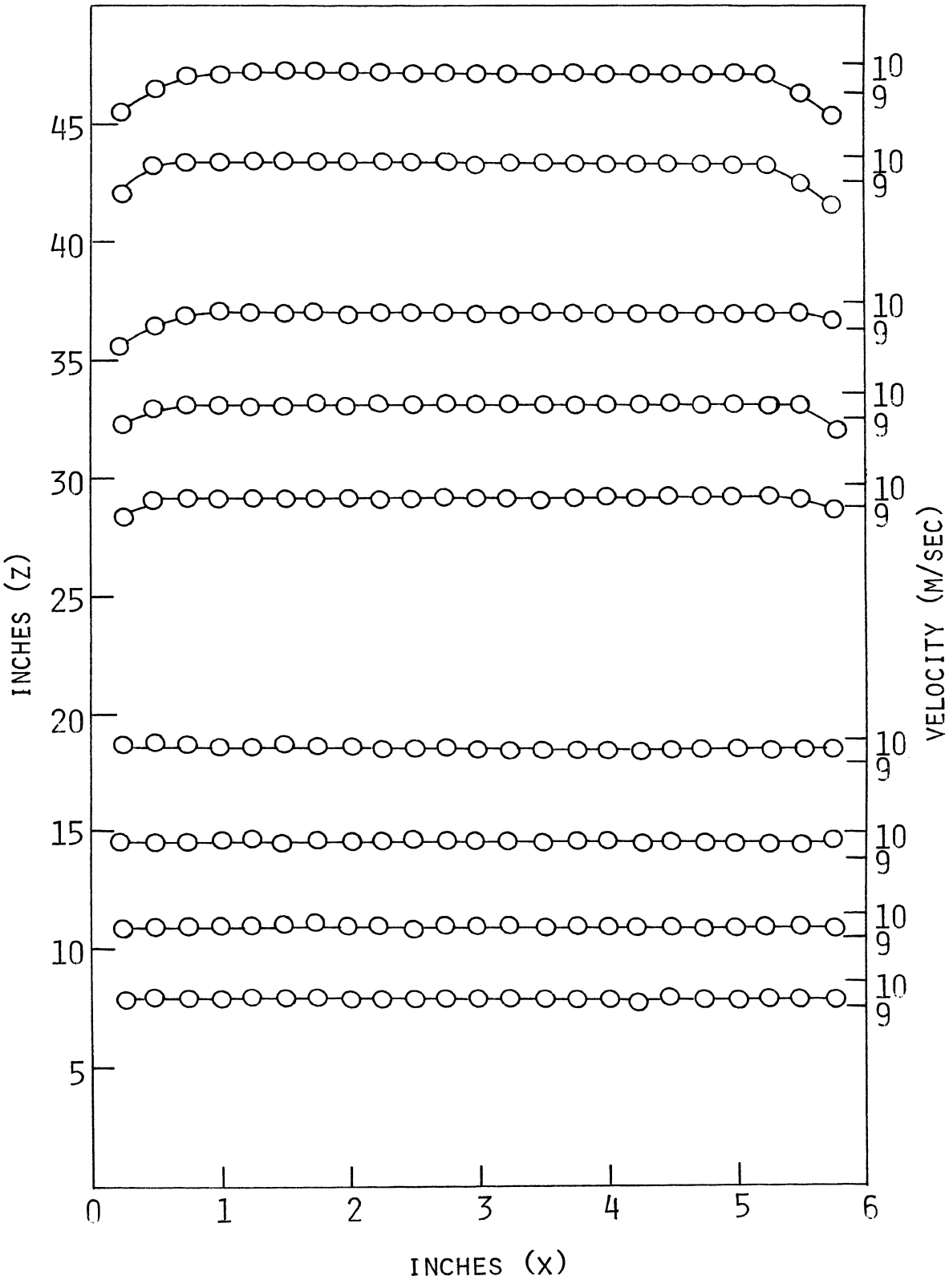

Figure 13. Mean Velocity Profile for U_o = 9.78 meters/sec.

up without accelerating the flow. In addition, to suspend a water droplet, it is essential that the average velocity be allowed to decrease slightly in the downstream direction for the purpose of maintaining vertical stability.

2. Turbulence Intensity

Stability of a suspended droplet is also a function of the momentary velocity of the flow field. An indication of this momentary velocity is the turbulence intensity. The smaller the turbulence intensity, the more stable the droplet can be suspended. Figures 14 and 15 show the turbulence intensity of the flow field between 11 and 40 inches downstream of the inlet to the test section for both one and two fans, respectively. Notice that in the center section of the test section the turbulence intensity is approximately below 0.5 per cent, which appears to be a reasonable indication of good stability.

In the boundary layer, the turbulence intensity data indicates that instability is to be expected whenever the droplet is within 1.5 inches of either wall.

3. Boundary Layer Thickness

The increase in the boundary layer can be seen from both the velocity distribution and turbulence intensity results. As shown in Figure 16, the boundary layer doesn't appear until the flow reaches the mid-section of the test section. This sudden generation of the boundary layer may largely be due to the friction generated by the surface roughness of the joints connecting the two test sections. Once the boundary layer develops, it begins to grow very rapidly, reaching 1.5 inches

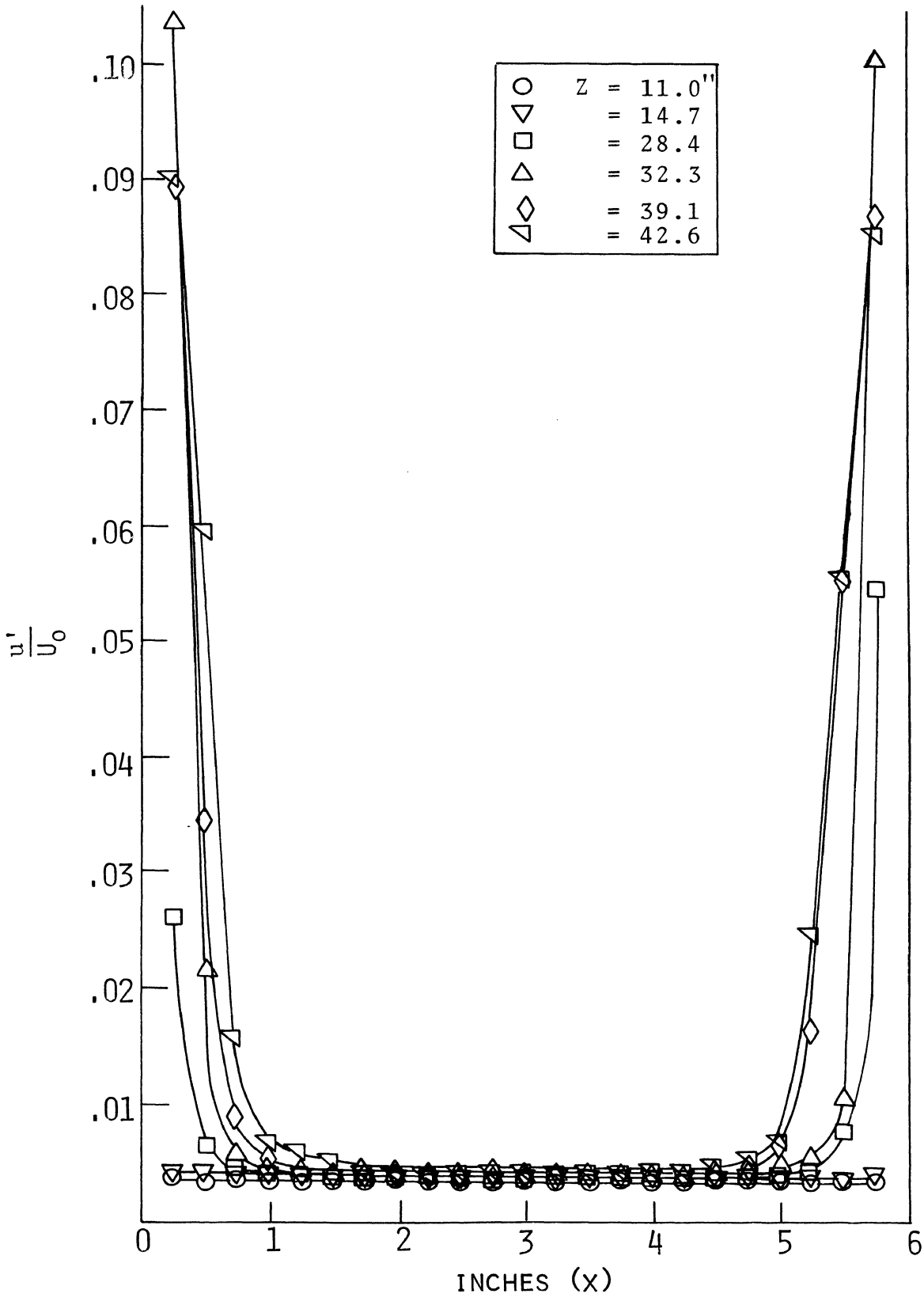

Figure 14. Longitudinal Turbulence Intensity for U_o = 6.15 meters/second

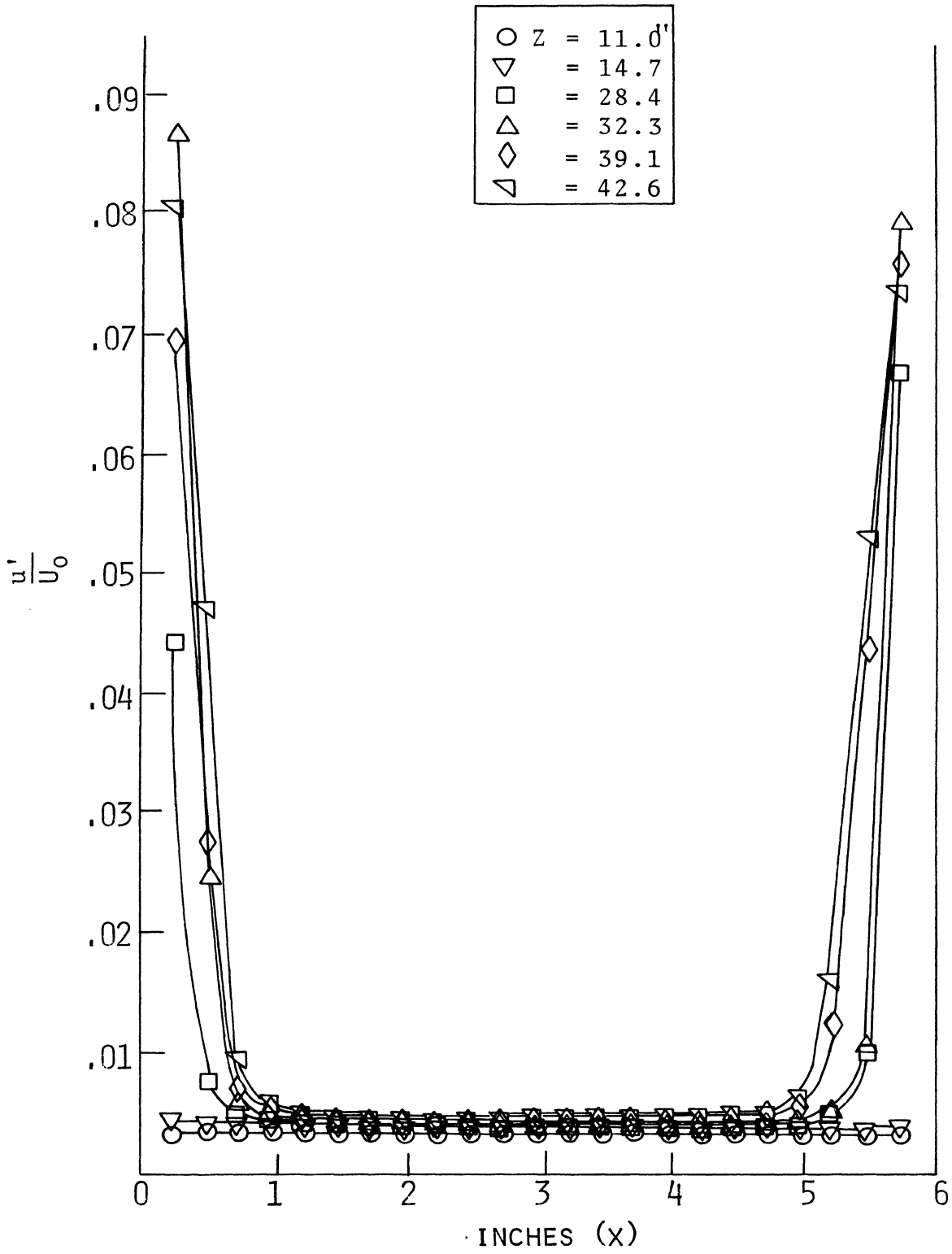

Figure 15. Longitudinal Turbulence Intensity for U_o = 9.78 meters/second

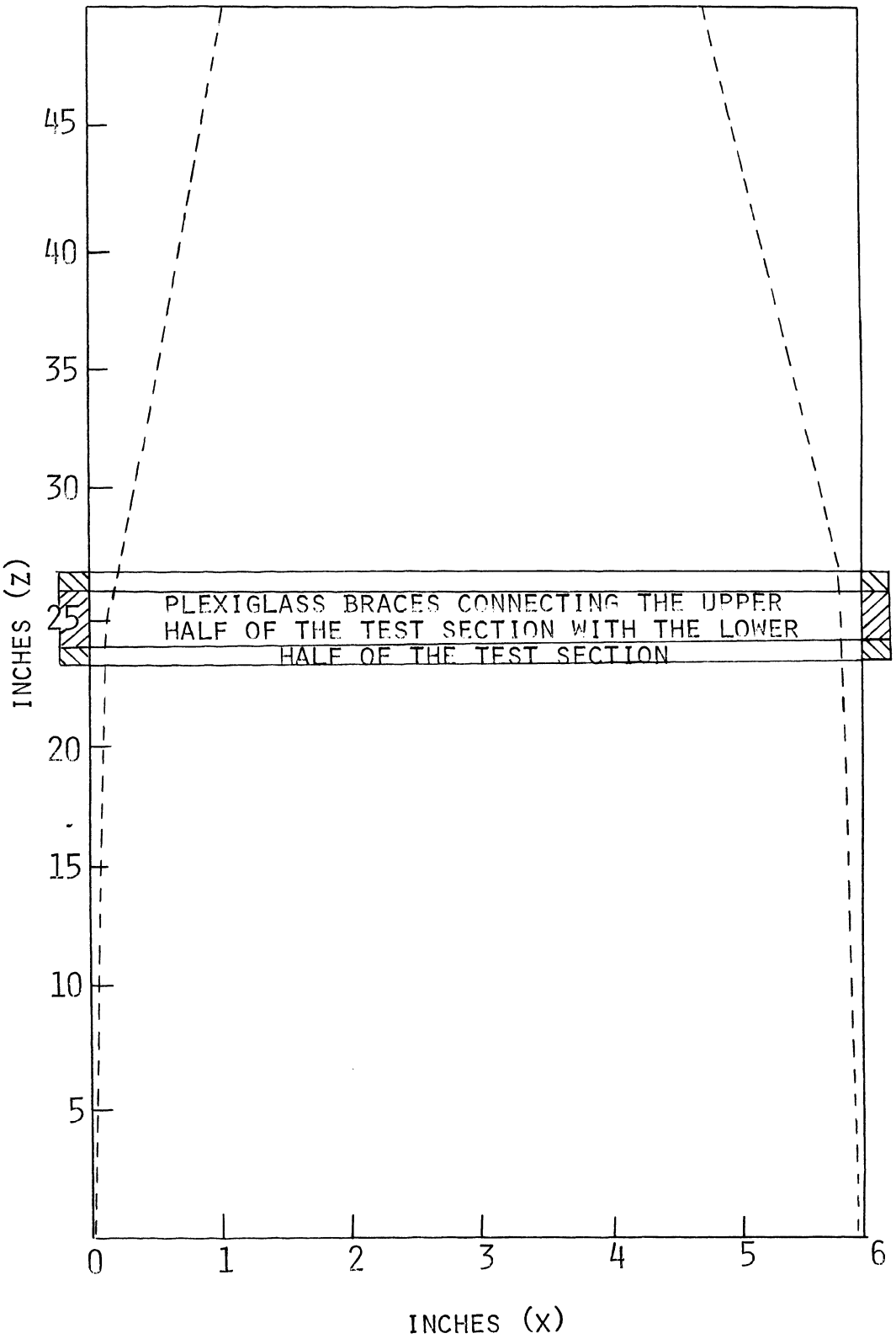

Figure 16. Boundary Layer Thickness for U_o = 6.15 m/sec

at the exit of the test section.

B. Turbulence Structure in the Wake of a Sphere

A solid sphere of 1.25 inches diameter was placed 11 inches downstream of the the test section inlet. Flow field characteristics were measured in both near wake regions and far wake regions for free stream velocities of 6.15 m/sec and 9.78 m/sec.

1. Near Wake Analysis

Mean velocity, turbulence intensity, and Reynolds shear stress measurements were made at 23 uniform locations, i.e., a measurement was made at every .25 inches while traversing from one wall of the test section to the other wall, for Z/D = 1.4 and Z/D = 3.0, where Z is the distance downstream from the center of the sphere and D is the diameter of the sphere. All values were non-dimensionalized with reference to the free stream velocity and graphically portrayed as a function of the radius from the center of the sphere divided by the diameter of the sphere.

a. Mean Velocity

Figure 17 shows the rapid decay of the mean velocity within the near wake of the sphere for 3 specific values of Z/D. At both 1.4 and 3.0 diameters (Z/D) downstream of the sphere, the boundary layer has not become thick enough to interact with the wake. However, at 11.4 diameters, the wake has dissipated such that the boundary layer has begun to affect the outer regions of the wake.

Differences in the mean velocity for Z/D = 1.4 and Z/D = 3.0 may be due to the pitot probe not being brought to pre-

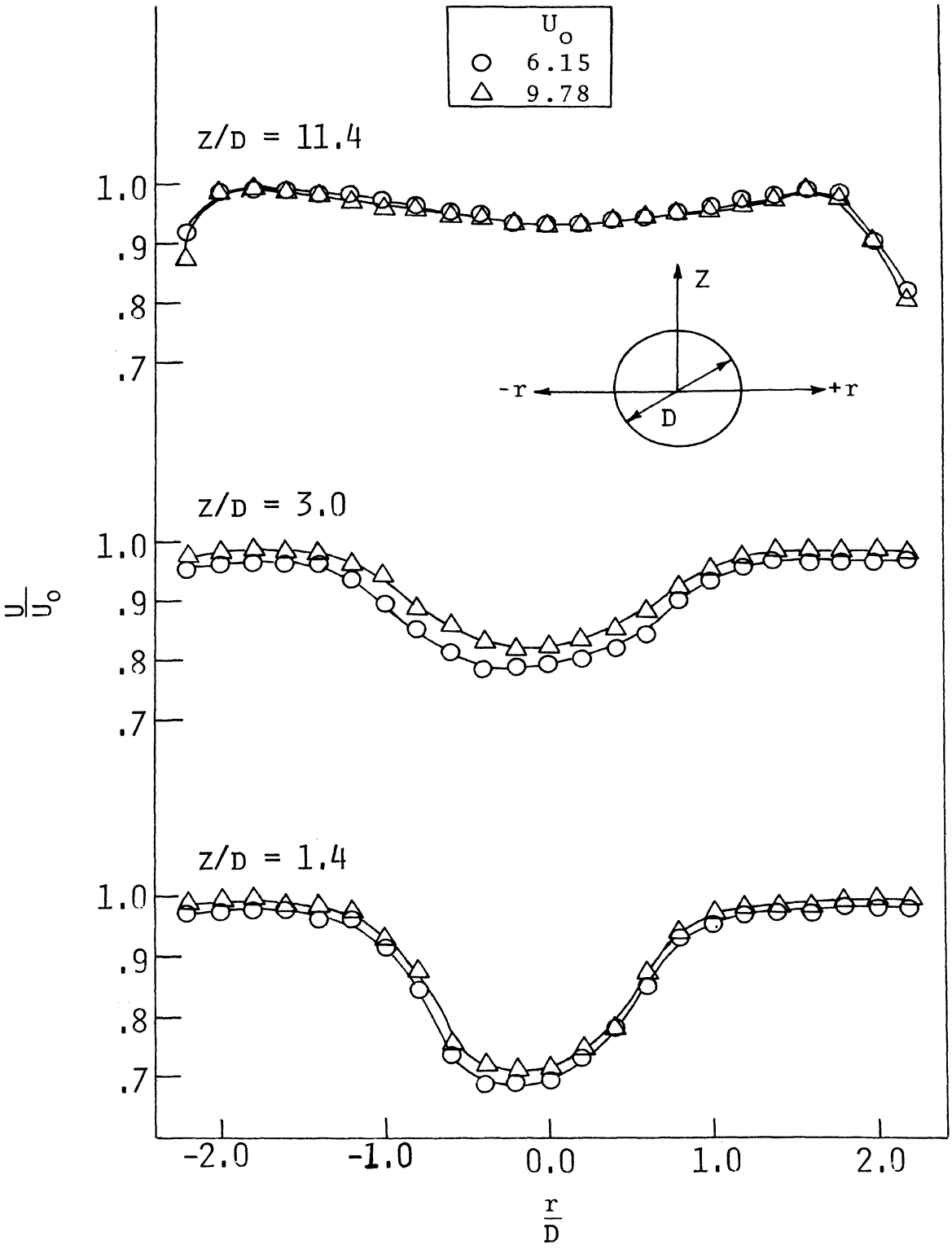

Figure 17. Mean Velocity Distribution Behind a Sphere for Z/D = 1.4, 3.0, and 11.4

cisely the same position for U_o = 9.78 m/sec as previously recorded for U_o = 6.15 m/sec.

Symmetry of the wake was checked by off-setting the probe 1 inch from the center of the sphere and traverses made in both the u_r and u_θ directions. Data showed that the centerline of the wake did not exactly coincide with the centerline of the sphere. This was due in part to the sphere being pulled slightly to one side of the tunnel by the stabilizing wires attached to the support rod.

b. Turbulence Intensity

Turbulence intensities were measured in the longitudinal, radial, and axial directions using an X-wire probe.

Figure 18 shows the longitudinal turbulence intensity to be relatively large at 1.4 diameters. At 3.0 diameters, the turbulence intensity has reduced approximately 50 per cent. At the beginning of the far wake region, Z/D = 11.4, the turbulence intensity has again dissipated by over 50 per cent. This indicates a very rapid dissipation of turbulence energy over a short distance behind the sphere. The slight variations of longitudinal turbulence intensity about the centerline again show that the flow was not exactly symmetrical with regard to the center of the sphere, but this was not considered a critical factor in the analysis.

Figures 19 and 20 show turbulence intensities for the radial and axial directions, respectively. At both 1.4 and 3.0 diameters, the intensities vary by a small amount. However, by the time the wake has reached 11.4 diameters, the intensities have decreased by over 50 per cent. This substantiates

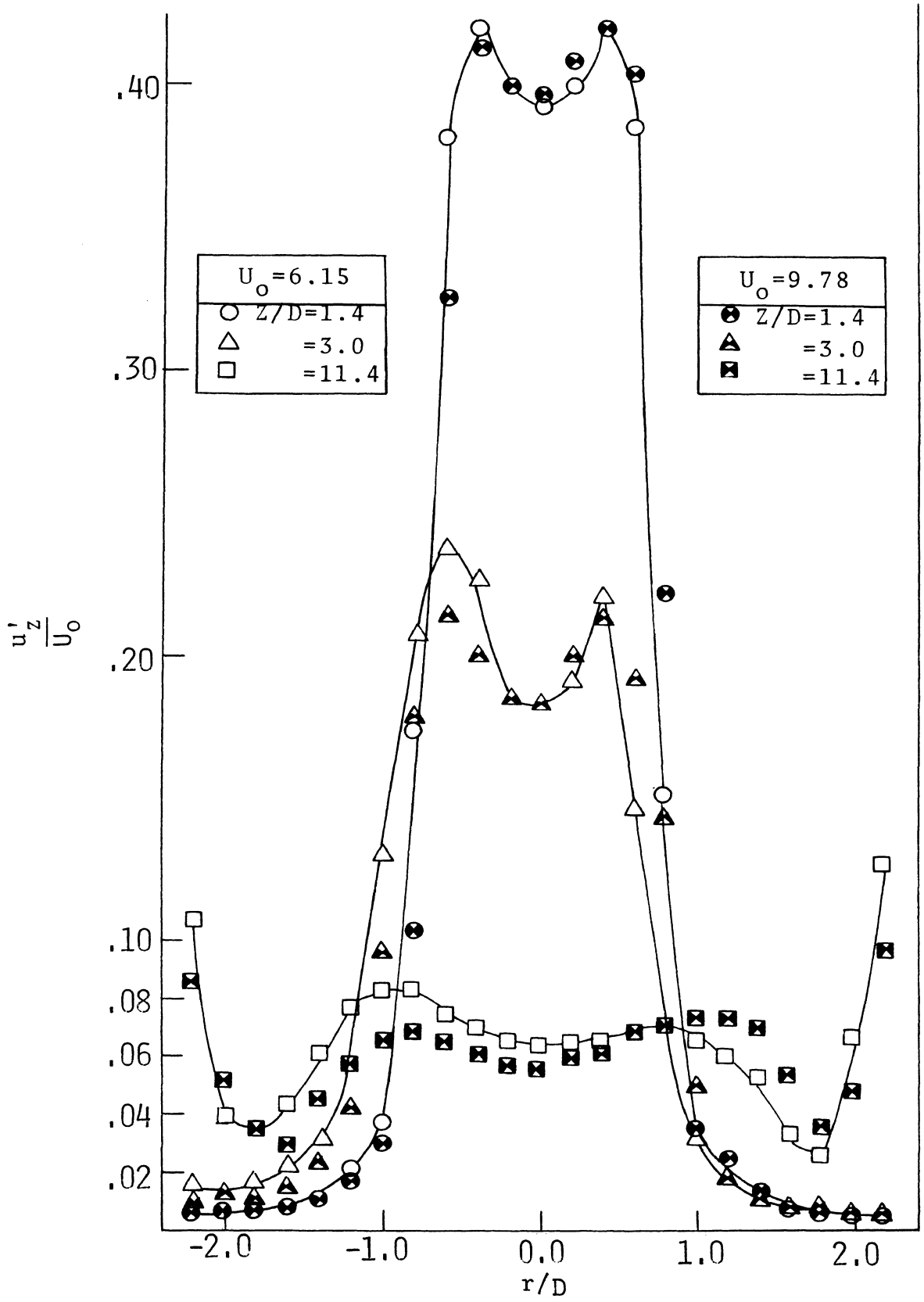

Figure 18. Longitudinal Turbulence Intensity for Z/D = 1.4, 3.0, and 11.4

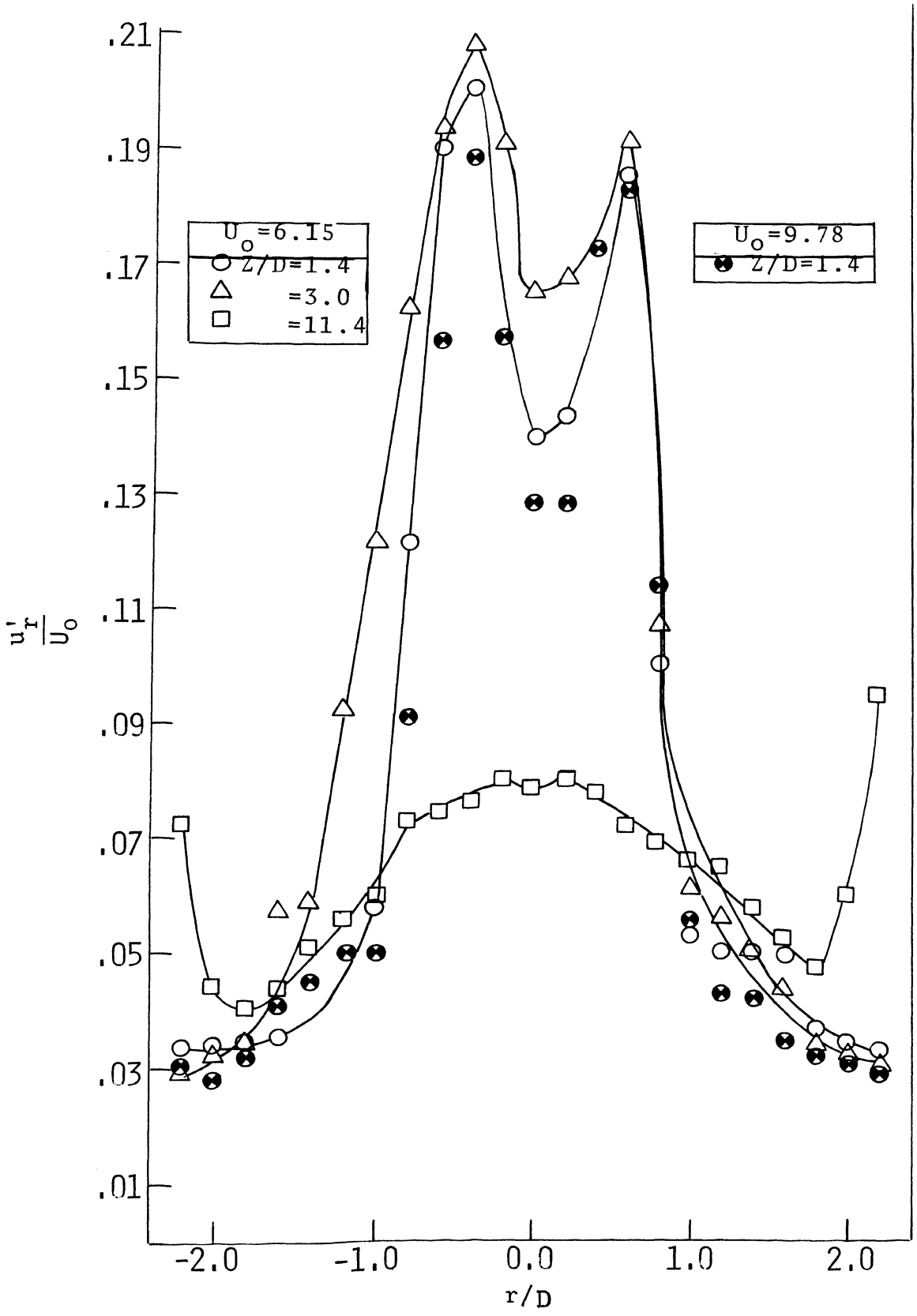

Figure 19. Radial Turbulence Intensity for Z/D = 1.4, 3.0, and 11.4

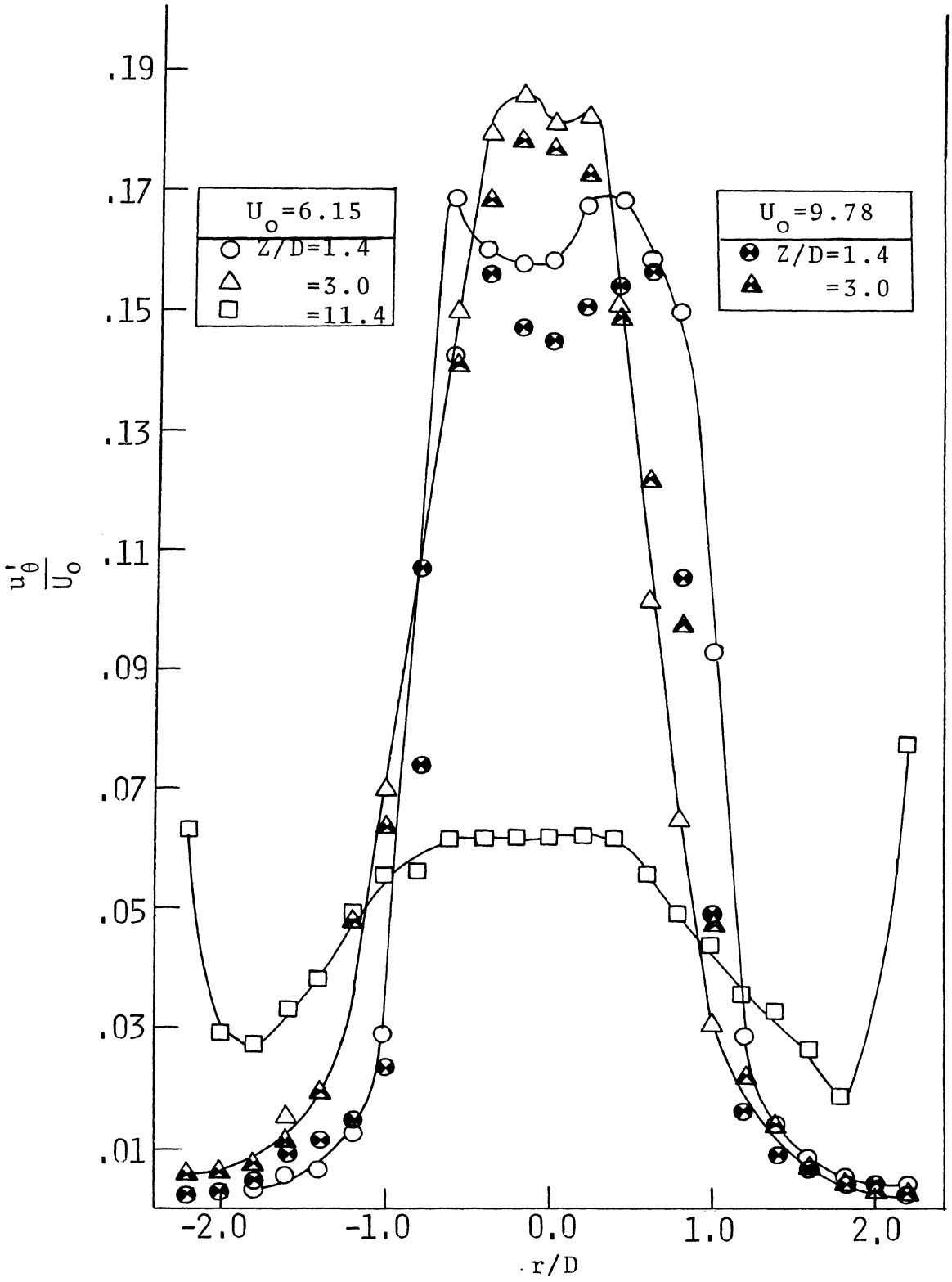

Figure 20. Axial Turbulence Intensity for Z/D = 1.4, 3.0, and 11.4

the results obtained from the longitudinal intensity measurements that the dissipation of turbulence energy occurs within 10 diameters downstream of the sphere. The axial component of turbulence intensity becomes small compared with the radial component in the outer edge of the mixing region. At 11.4 diameters, the wake has dissipated greatly and both components of turbulence intensity approach the same value.

c. Reynolds Shear Stress

Figures 21 and 22 show double correlation measurements for the longitudinal-radial direction and the longitudinal-axial direction, respectively. At 1.4 diameters, shear stress values for both axial and radial correlations are approximately equal, and show that there is a finite region where turbulent mixing occurs. The axial correlation value decreases rapidly within the near wake region while the radial correlation value remains large. Consequently, more measurements need to be taken between 3.0 and 11.4 diameters to fully ascertain the decay of the radial shear stresses.

Boundary layer effects begin to appear at 11.4 diameters. Shear stresses appear symmetrical but not identical in value about the centerline of the wake.

The large values for the longitudinal-radial stresses account for the large values of radial turbulence intensity. This indicates that as the fluid flows around the sphere, a larger amount of fluid is displaced in the radial direction than in the axial direction within the dissipation zone of turbulence

2. Far Wake Analysis

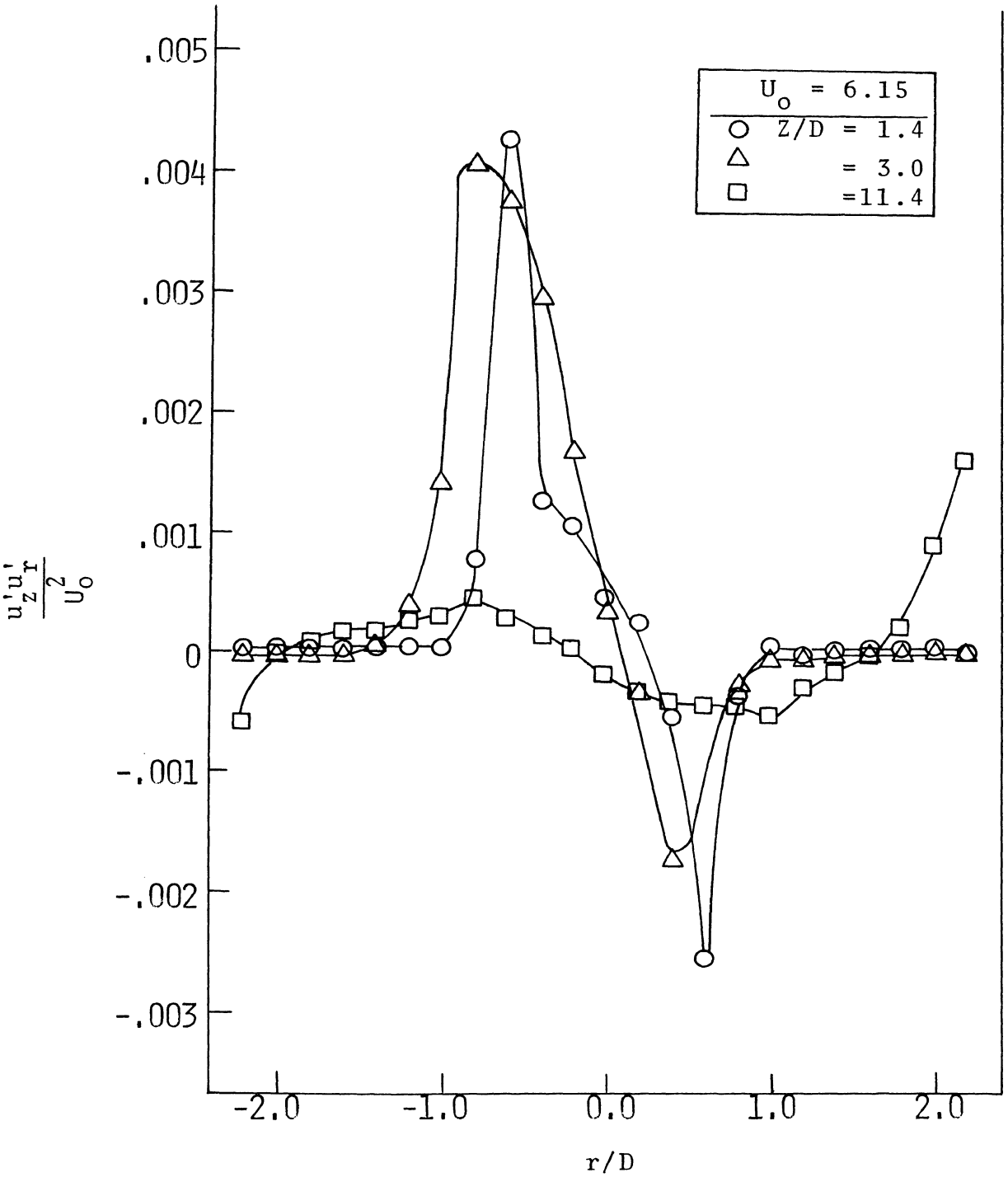

Figure 21. Longitudinal-radial shear stress for Z/D = 1.4, 3.0, and 11.4

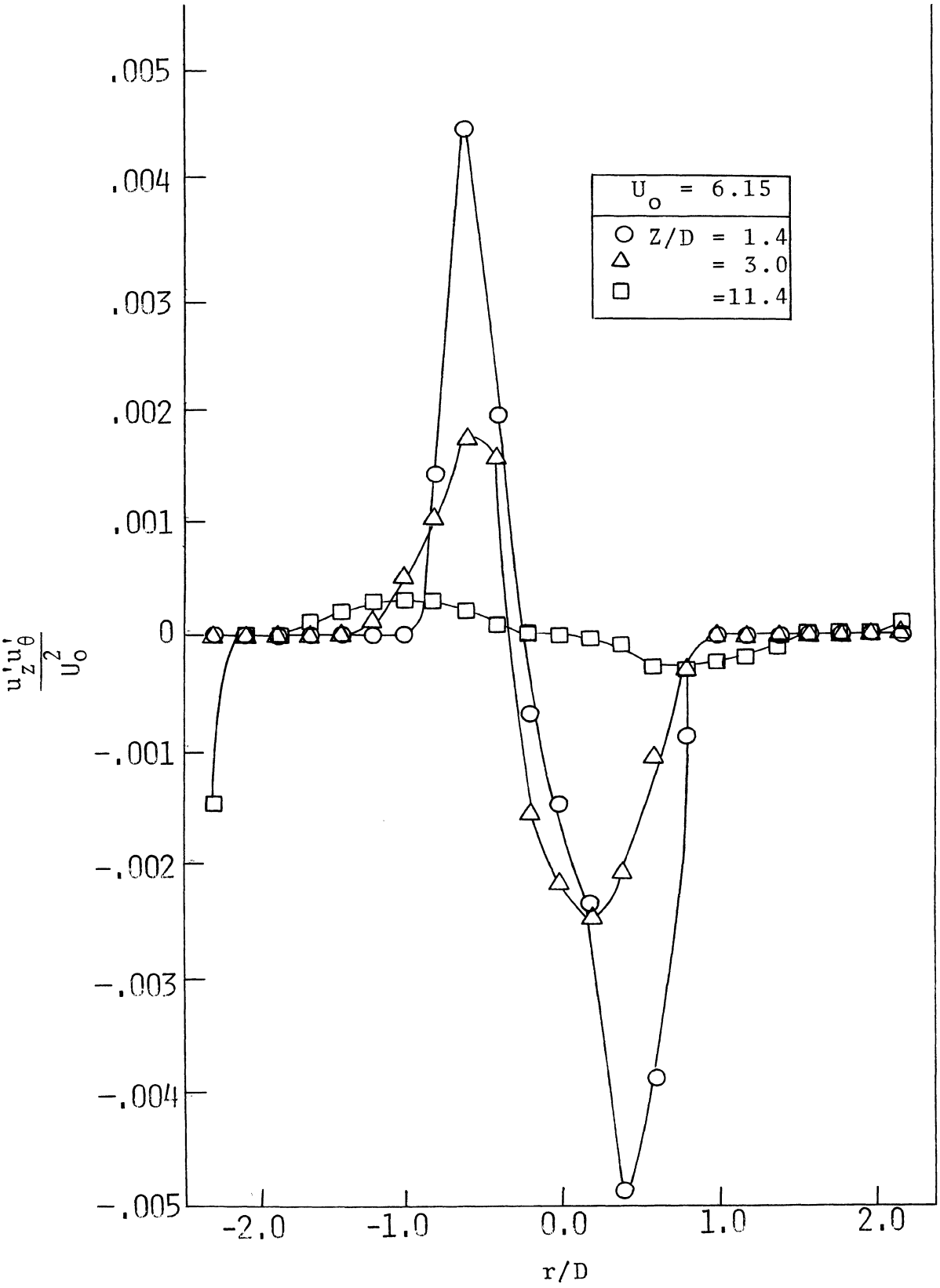

Figure 22. Longitudinal-axial shear stress for Z/D = 1.4, 3.0, and 11.4

Four traverses were made in the far wake region of the sphere for Z/D = 15.6, 18.6, 21.2, and 24.0. Mean velocity, turbulence intensity, and shear stress measurements were recorded for both free stream velocities as were previously measured for the near wake region.

a. Mean Velocity

Figure 23 shows the steady decay of the wake as the flow progresses to 24 diameters downstream of the sphere. The interaction of the wake with the boundary layer becomes predominant beyond 15 diameters, due to the centerline of the wake drifting to the left wall of the tunnel (r/D = - 1.0).

The slight differences in the mean velocities as seen in Figure 23, particularly within the boundary layer profiles, may be attributed to the fact that the pitot-static probe was not exactly in the same location for U_o = 9.78 m/sec as it was for U_o = 6.15 m/sec.

b. Turbulence Intensity

Figures 24, 25, and 26 show the longitudinal, radial, and axial turbulence intensities, respectively.

The interaction between the wake and free stream flow is quite distinct at 15.6 diameters for the longitudinal intensity, shown in Figure 24. Decay of the wake continues slowly between 18.6 and 24.0 diameters, supporting previous results that there is a very rapid establishment and dissipation of the wake behind a sphere. At 24.0 diameters the values of longitudinal turbulence intensity have nearly reached those of the background turbulence previously recorded for the test section.

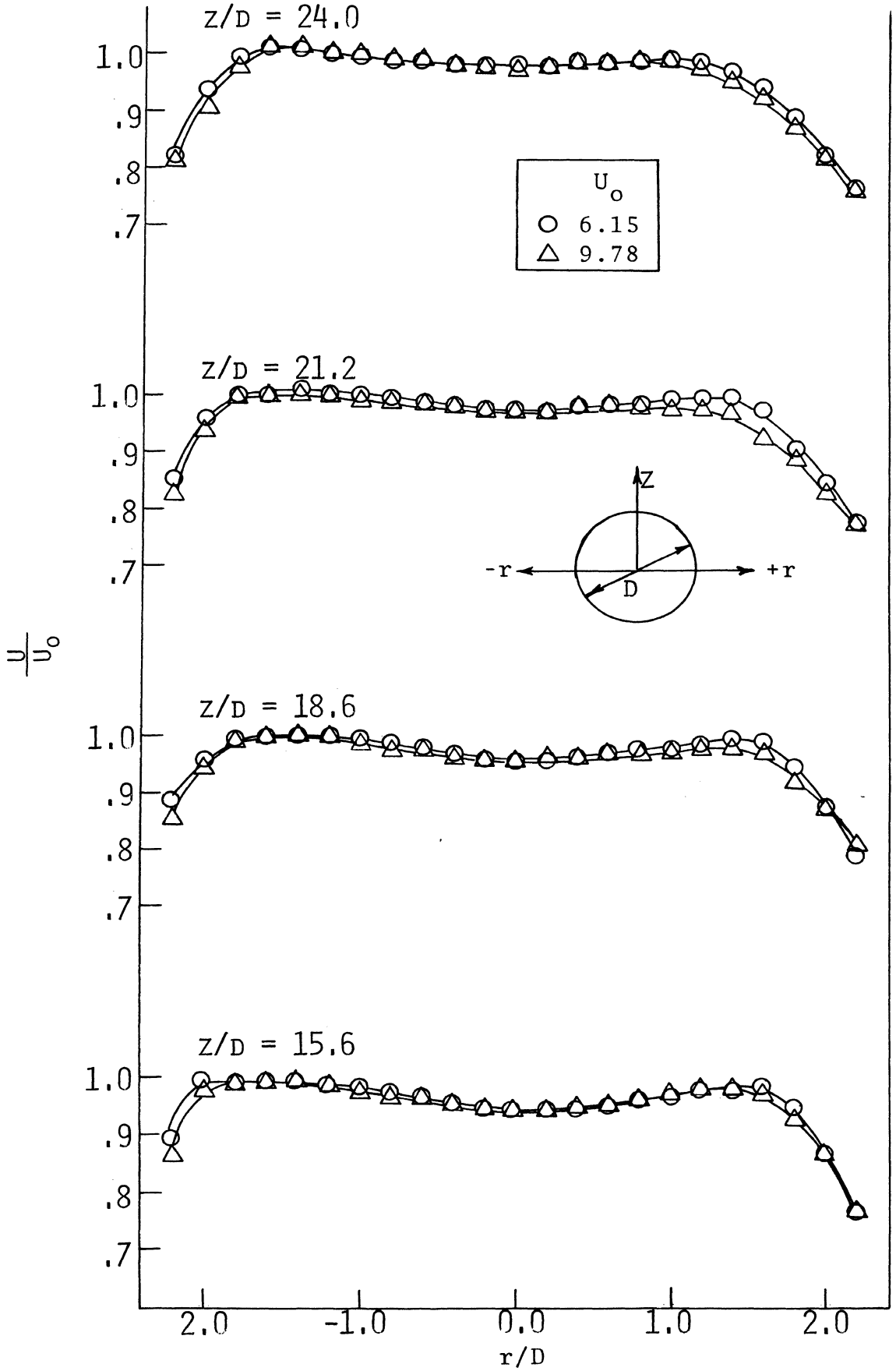

Figure 23. Mean Velocity profiles for Z/D = 15.6, 18.6, 21.2, and 24.0

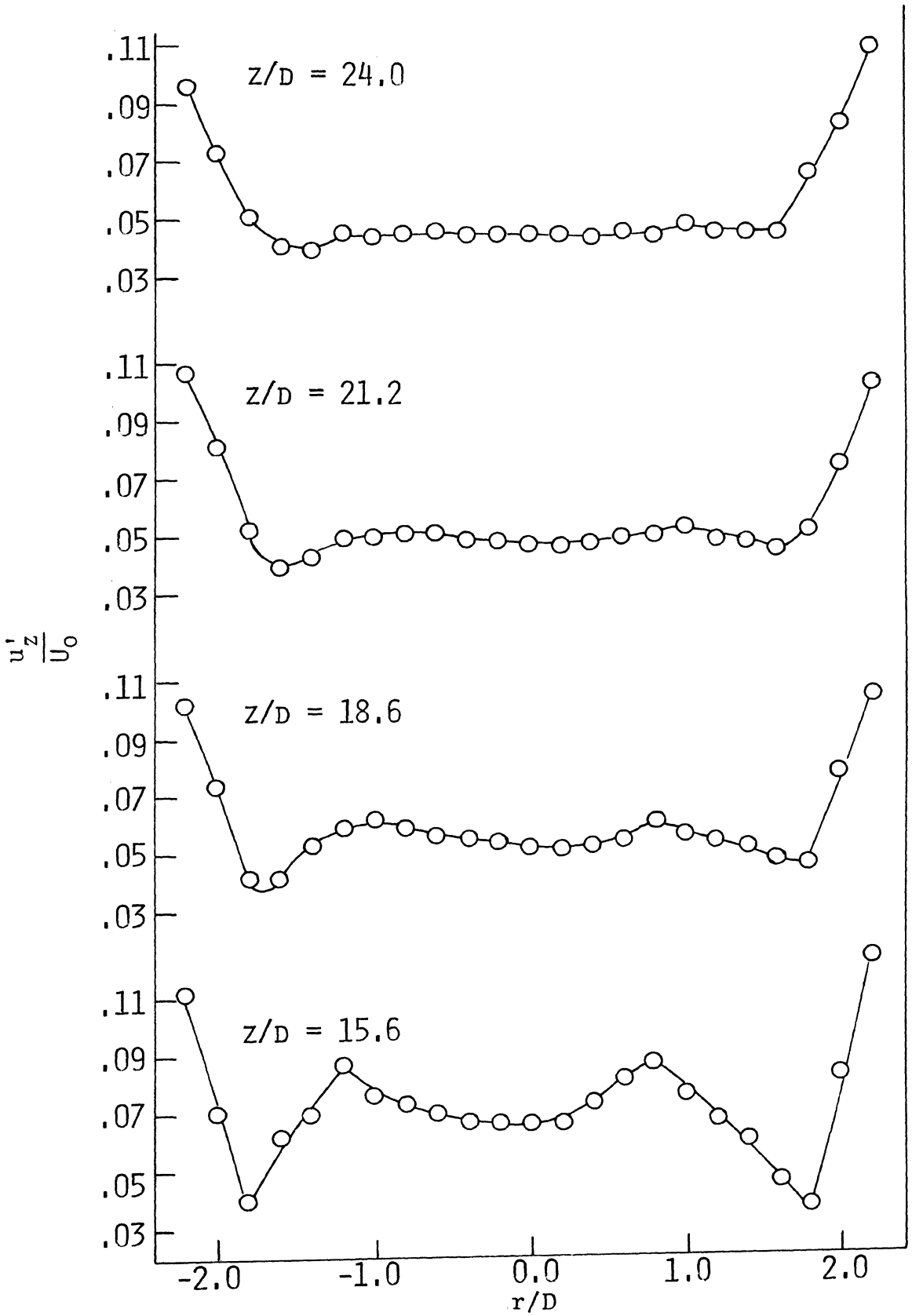

Figure 24. Longitudinal Turbulence Intensity for Z/D = 15.6, 18.6, 21.2, and 24.0

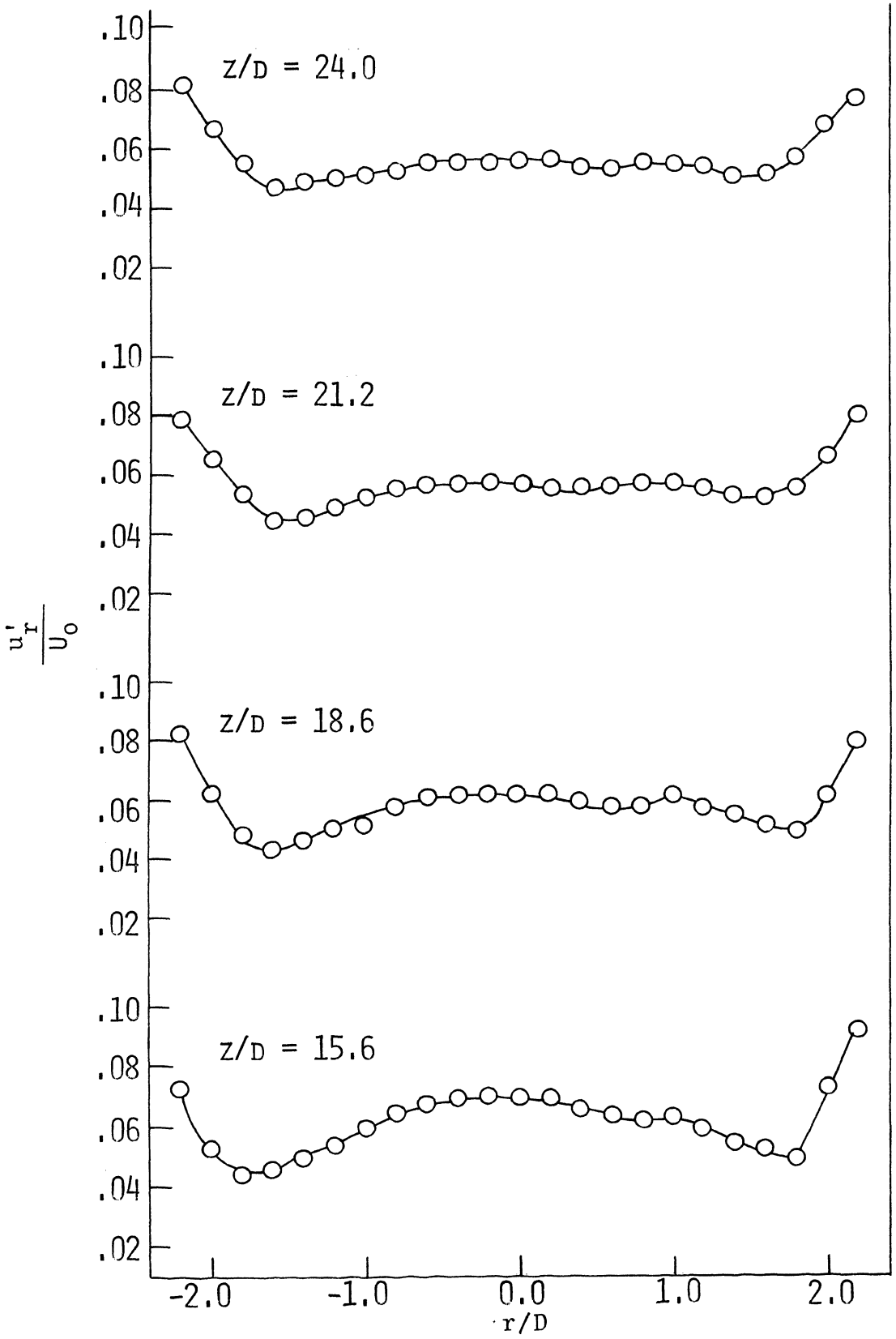

Figure 25. Radial Turbulence Intensity for Z/D = 15.6, 18.6, 21.2, and 24.0

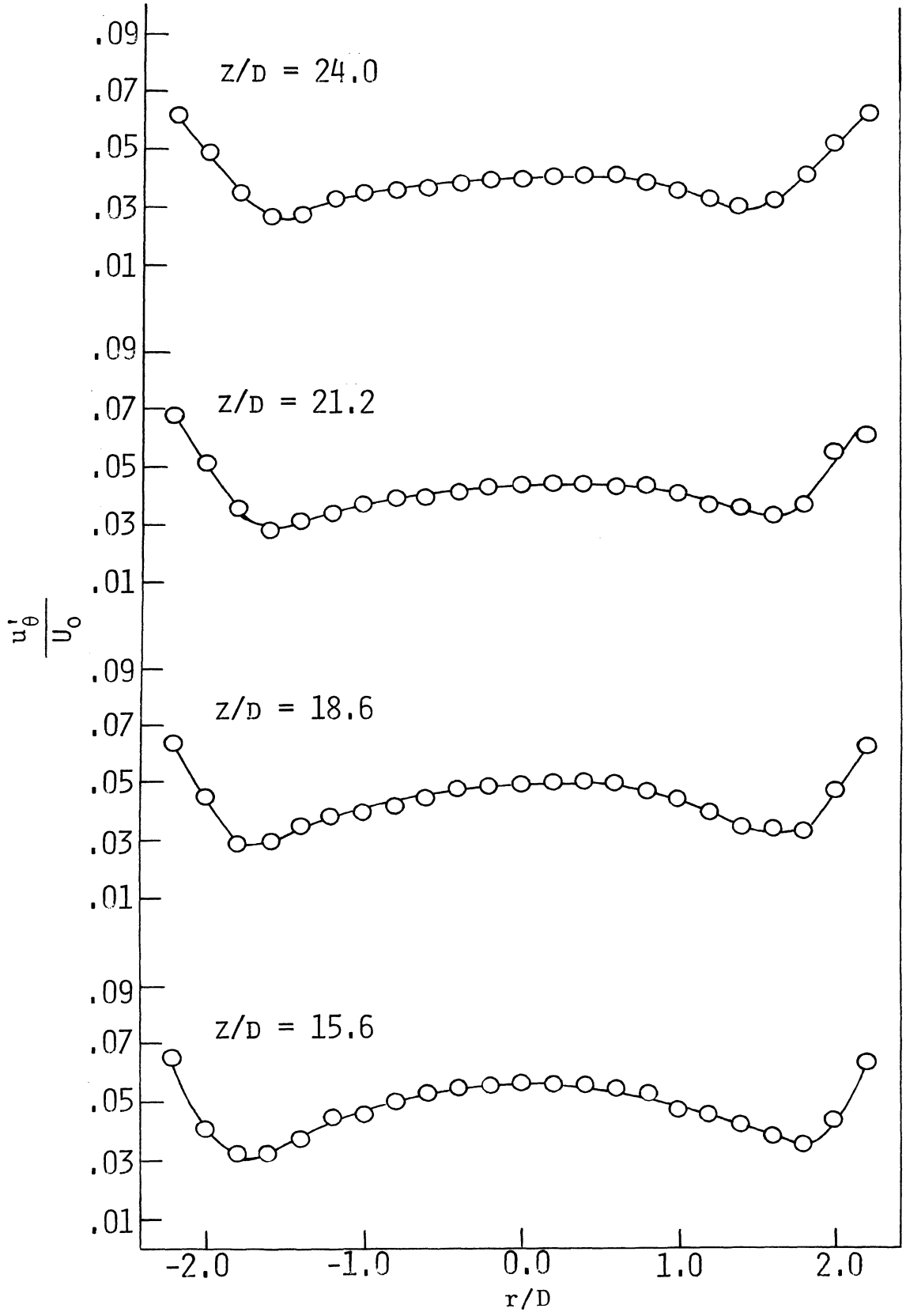

Figure 26. Axial Turbulence Intensity for Z/D = 15.6, 18.6, 21.2, and 24.0

Figures 25 and 26 show the turbulence intensities in both the radial and axial directions to be approximately equal. The similarity of these intensities suggests that the turbulent eddies generated in the near wake break up and attain a rather consistent orientation very early. Notice that the turbulence intensity in either the radial or axial direction has not quite reached a steady value at 24.0 diameters as was the case in the longitudinal direction.

c. Reynolds Shear Stress

Figures 27 and 28 show that the longitudinal-axial shear stresses decrease very gradually to a constant value for free stream conditions. The shear stress profile spreads significantly as the wake progresses downstream. The influence of the wall shear stresses upon the free shear stresses becomes evident around 15 diameters. This accounts for the irregularity of the shear stress profiles just outside the boundary layer region of the walls.

Figures 29 and 30 show values of radial shear to be slightly larger than the axial shear of Figures 27 and 28. Scale expansions show the shear stress in the far wake region for the longitudinal-radial correlation decreasing slowly with increasing distance from the center of the sphere and dissipating outward. In addition the shear in the radial direction is more irregular than the shear in the axial direction, and indicates that there may be a small irregular cross-flow in the tunnel, possibly due to flow leakage around the joints of the test section.

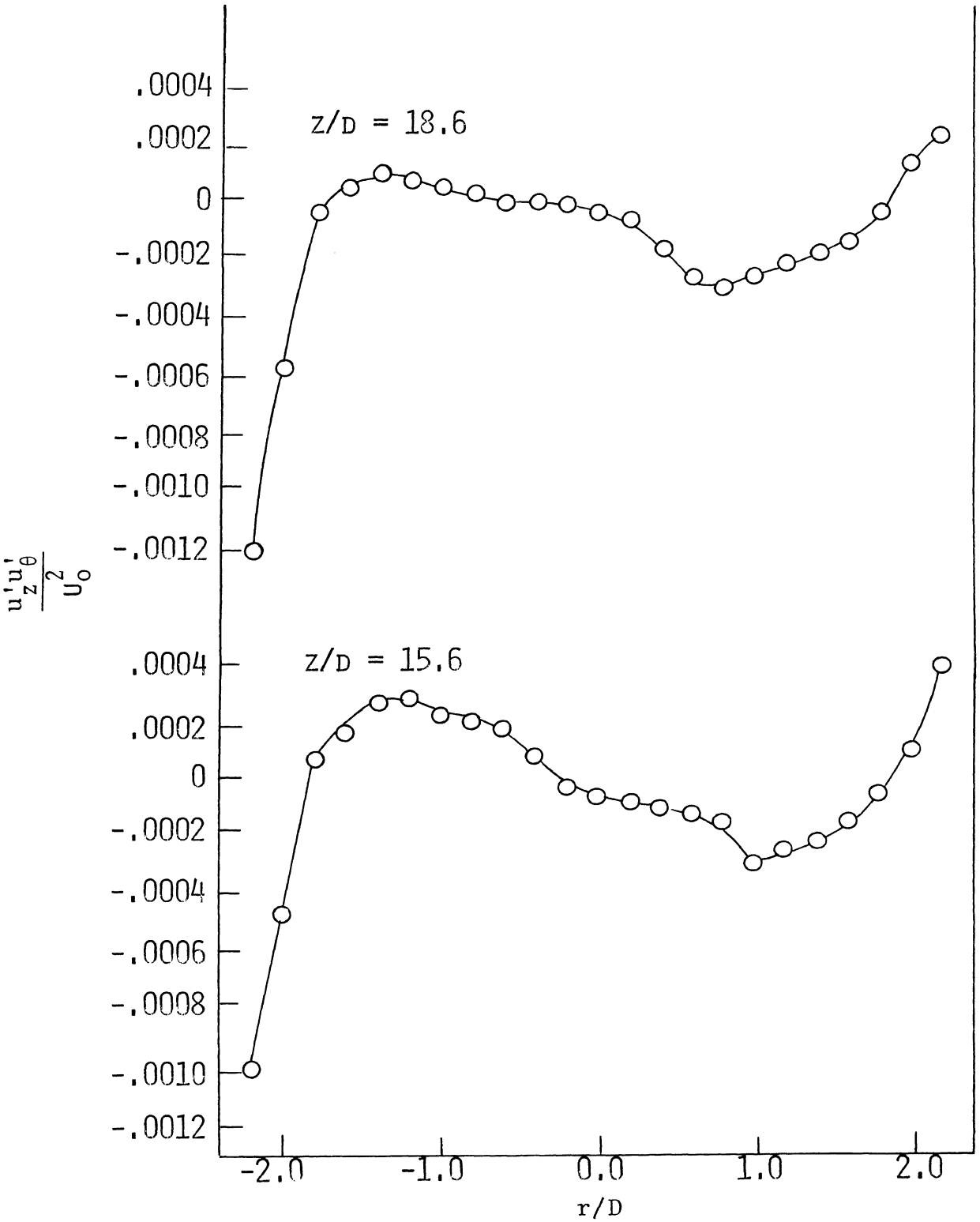

Figure 27. Longitudinal-axial shear stress for Z/D = 15.6 and 18.6

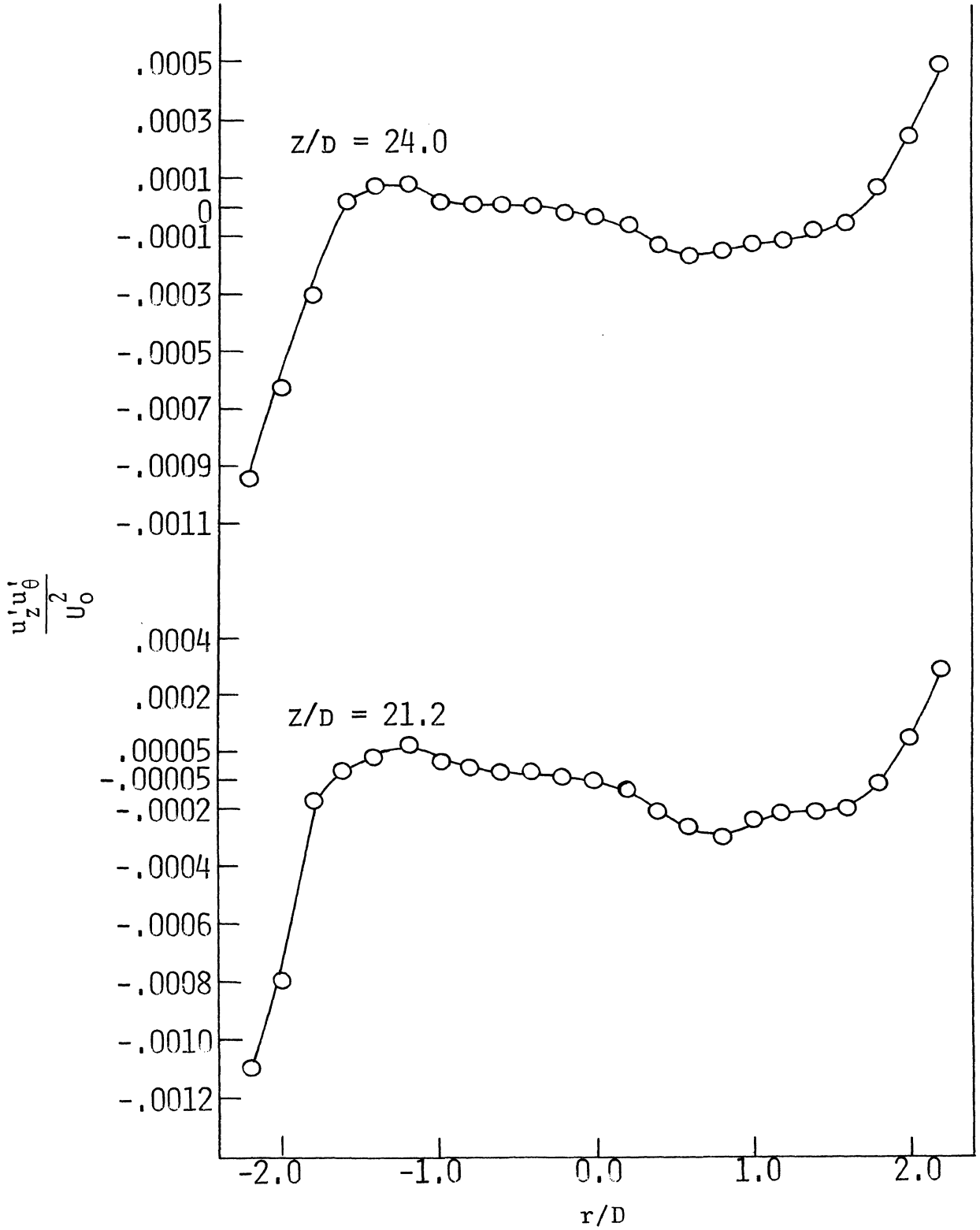

Figure 28. Longitudinal-axial shear stress for Z/D = 21.2 and 24.0

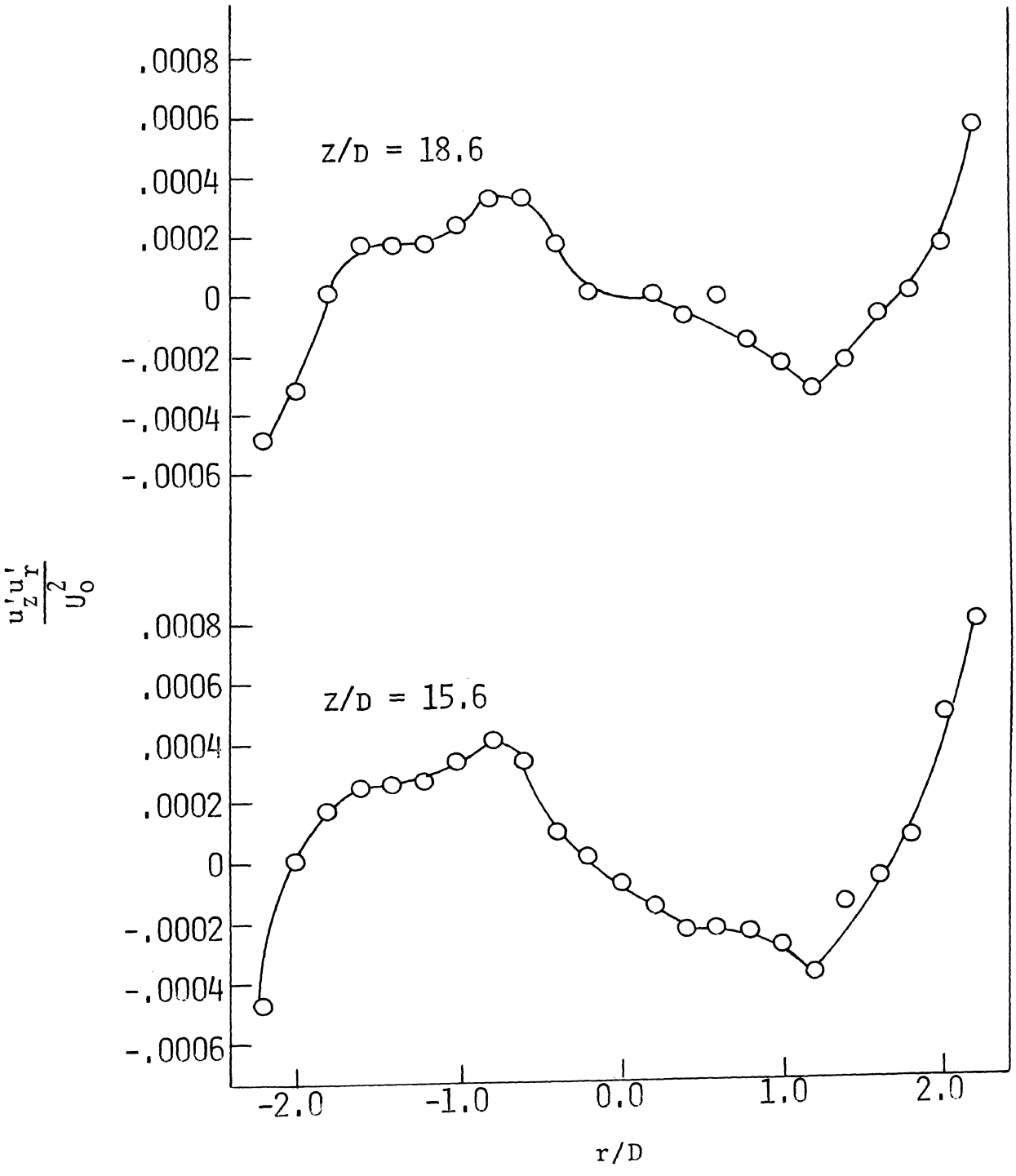

Figure 29. Longitudinal-radial shear stress for Z/D = 15.6 and 18.6

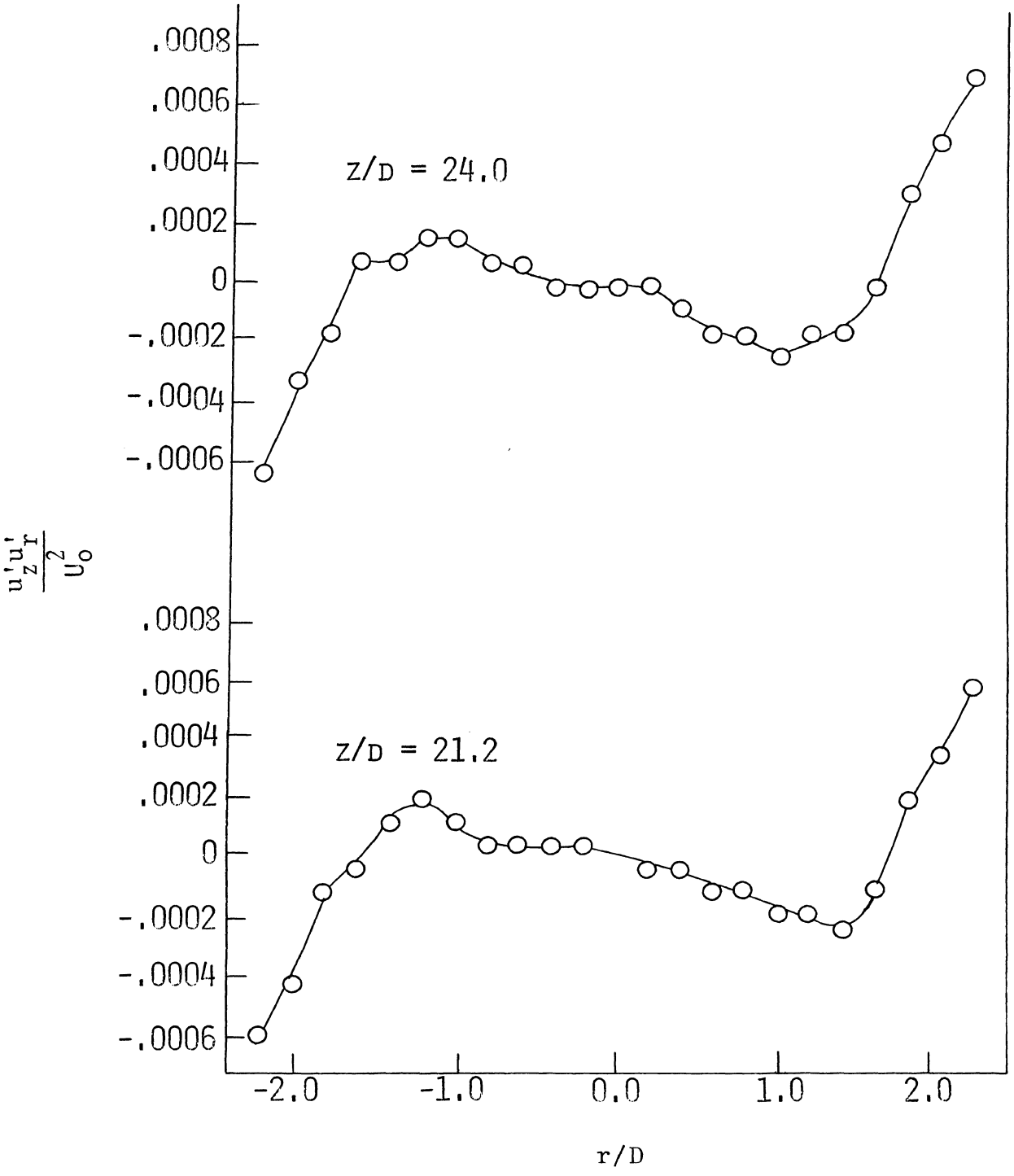

Figure 30. Longitudinal-radial shear stress for Z/D = 21.2 and 24.0

VI. CONCLUSION

The UMR Vertical Atmospheric Wind Tunnel appears to be a suitable, low turbulence generating system with adequate capabilities for conducting experiments dealing with small droplets. The background turbulence of the system is low and does not influence the behavior of a suspended droplet.

The boundary layer grows within a 6 inch vertical section beginning at Z = 18 inches. This rapid boundary layer growth tends to disrupt the stability of the suspended droplet within the downstream section of the wind tunnel. In order for the droplet to remain stabily suspended, the droplet should be injected into the lower half of the test section, or a diverging section incorporated in the upper half of the test section.

Pressure profiles show that the free tunnel velocity is very uniform for any cross-section throughout the entire length of the test section. The turbulence remains fairly constant for increasing distances from the inlet of the test section. At U_o = 9.78 m/sec, the turbulence in the free stream of the tunnel decreases very little compared with U_o = 6.15 m/sec. The mean velocity, however, increases significantly due to the effect of the boundary layer thickness, i.e., fully developing flow.

Near wake results show turbulence intensities to be very high downstream of the sphere, but are somewhat questionable for values of turbulence recorded at 1.5 diameters. The fact that the turbulence within the wake dissipated to within 20

per cent of its maximum value at 10 diameters indicates that the wake becomes established within a very limited zone.

Chevray (8) points out that the flow behind an oblate spheroid (body of revolution) becomes established at a section located between 3 and 6 diameters downstream of the spheroid while Carmody (10) finds the flow behind a disk to be established within 15 diameters. The flow behind a sphere should become established between 6 and 15 diameters. Experimental results show that the establishment of the wake behind a sphere occurs at 11 diameters.

The last few far wake profiles show the influence of the wall shear stresses over the free shear stresses. The boundary layer grows so rapidly that it inneracts with the wake at 15 diameters. The radial shear stress shows the effects of this inneraction whereby values were nearly 10 times larger than the values measured for the axial shear stress. A much larger test section should be used in order to insure good repeatable results, in addition to reducing disturbance of the wake from external sources.

Irregularities about r/D = 0.0 show that the wake "centerline" was not exactly at the center of the sphere. The wake tended to drift noticeably to one side of the tunnel due to improper alignment of the test model. However, data was adequate for analyzing the wake development before interference with the boundary layer occurred.

VII. BIBLIOGRAPHY

1. Pruppacher, H. R. and Beard, K. U. (1969), "A Determination of the Terminal Velocity and Drag of Small Water Drops by Means of a Wind Tunnel," Journal of the Atmospheric Sciences, 26, p. 1066-1072.

2. Field, L. V. (1970), "Design and Construction of a Velocity Control System for a Low Turbulence Vertical Wind Tunnel," M. S. Thesis, University of Missouri - Rolla, 48 p. (with 12 figures).

3. Squires, P. (1968), "The Growth of Droplets in Warm Clouds," Proceedings of the International Conference on Cloud Physics, p. 57.

4. Townsend, A. A. (1947), "Measurements in the Turbulent Wake of a Cylinder," Proceedings of the Royal Society, London, Ser A, Vol. 190, p. 551-561.

5. Hinze, J. O. (1959), Turbulence, McGraw-Hill.

6. Sami, S. (1966), "Velocity and Pressure Fields of a Diffusing Jet," Ph. D. Dissertation, University of Iowa, 99 p. (with 50 figures).

7. Naudascher, E. (1965), "Flow in the Wake of Self-Propelled Bodies and Related Sources of Turbulence," Journal of Fluid Mechanics, Vol. 22, Part 4, p. 625-656.

8. Chevray, R. (1968), "Turbulent Wake of a Body of Revolution," Journal of Basic Engineering, June, p. 257-284.

9. Schlichting, H. (1968), Boundary Layer Theory, 6th. Edition, McGraw-Hill.

10. Carmody, T. (1964), "Establishment of the Wake Behind a Disk," Journal of Basic Engineering, Trans. ASME, Series D, Vol. 87, No. 4, December, p. 869-882.

11. DISA (1969), "Instruction and Service Manuel for Type 55D01 Anemometer Unit."

12. Abraham, F. F. (1968), "A Physical Interpretation of the Structure of the Ventilation Coefficient for Freely Falling Water Drops," Journal of the Atmospheric Sciences 25, p. 76-81.

13. Holder, D. W. and Pankhurst, R. C. (1952), Wind Tunnel Technique, Issaac Pitman and Sons, Ltd.

14. Hoffer, T. E. and Mallen, S. C. (1968), "A Vertical Wind Tunnel for Small Droplet Studies," Journal of App. Meteorology, Vol. 7, p. 290-292.

15. Cooper, R. D. and Tulin, M. P. (1955), "Turbulence Measurements with the Hot-wire Anemometer," North Atlantic Treaty Organization Advisory Group for Aeronautical Research and Development."

16. Pruppacher, H. R. and Neiburger, M. (1968), "Design and Performance of the UCLA Cloud Tunnel," Proceedings of the International Conference on Cloud Physics, p. 389-391.

17. Keffer, J. F. (1965), "The Uniform Distortion of a Turbulent Wake," Journal of Fluid Mechanics, Vol. 22, Part 1, p. 135-159.

18. Mason, B. J. and Woods, J. D. (1964), "The Wake Capture of Water Drops in Air," Quarterly Journal of the Royal Meteorological Society 90, p. 35-43.

19. Jeffrey, R. C. and Pearson, J. R. A. (1965), "Particle Motion in Laminar Vertical Tube Flow," Journal of Fluid Mechanics, Vol. 22, Part 4, p. 721-735.

20. Heskestad, G. (1965), "Hot-wire Measurements in a Plane Turbulent Jet," Journal of Applied Mechanics, December, p. 721-734.

VITA

The author, Darrell Weldon Pepper, was born on May 14, 1946, in Kirksville, Missouri.

He graduated from Pattonville High School, St. Ann, Missouri, in June, 1964, and entered the University of Missouri at Rolla in September, 1964. He received the degree of Bachelor of Science in Mechanical Engineering in 1968, and is a member of Pi Tau Sigma Honorary Mechanical Engineering Fraternity.

He enrolled in the Graduate School of the University of Missouri - Rolla in September, 1968, and worked as a graduate assistant in the Department of Mechanical and Aerospace Engineering until June, 1969.

The author joined the Graduate Center for Cloud Physics Research in June, 1969, and has worked as a research assistant until the present time under THEMIS Contract N0014-68-A-0497 (2357-2228).

APPENDIX A: TURBULENT FLOW EQUATIONS

Turbulent motion can be characteristics by its mean, or average, value of velocity and by a measure of its fluctuating velocity, or violence of motion. The momentary value of velocity is a function of both the mean and fluctuating values of velocity and is given by the equation

$$U = \overline{U} + u$$

Density and pressure are also considered to consist of a mean value plus a fluctuating value, as given by

$$P = \overline{P} + p$$

$$\rho = \overline{\rho} + \rho'$$

If the turbulent flow field is assumed to be quasi-steady, that is, the characteristic features of the turbulent flow appear to be irregular and disorderly, the momentary values of velocity, pressure, and density must be averaged with respect to time. This concept of time averaging is used in deriving the turbulent continuity, momentum, and energy equations.

I. Continuity Equation

The continuity equation can be written in terms of a momentary value of velocity as

$$\frac{\partial}{\partial X_i} (\overline{U}_i + u_i) = 0 \qquad \text{(A-1)}$$

Averaging with respect to time gives

$$\frac{\partial}{\partial X_i} \overline{(\overline{U}_i + u_i)} = 0$$

which reduces to

$$\frac{\partial}{\partial X_i} \overline{U}_i = \frac{\partial}{\partial X_i} \overline{U}_i = 0 \qquad \text{(A-2)}$$

II. Momentum Equation for Turbulent Flow

The momentum equation, with momentary values of density, pressure, and velocity, is written as

$$(\overline{\rho} + \rho')(\overline{U}_j + u_j)\frac{\partial}{\partial X_j}(\overline{U}_i + u_i) = (\overline{F}_i + f_i) - \frac{\partial}{\partial X_i}(\overline{P} + p) + \mu\left[\frac{\partial^2}{\partial X_j \partial X_j}(\overline{U}_i + u_i) + \frac{\partial^2}{\partial X_i \partial X_j}(\overline{U}_j + u_j)\right] \quad (A\text{-}3)$$

Averaging with respect to time, the left hand side of equation (A-3) becomes

$$\overline{\rho}\overline{U}_j\frac{\partial}{\partial X_j}\overline{U}_i + \overline{\rho u_j\frac{\partial u_i}{\partial X_j}} + \overline{\rho' u_j}\frac{\partial}{\partial X_j}\overline{U}_i + \overline{\rho' u_j\frac{\partial u_i}{\partial X_j}} + \overline{U}_j\overline{\rho'\frac{\partial u_i}{\partial X_j}}$$

while the right hand side becomes

$$\overline{F}_i - \frac{\partial \overline{P}}{\partial X_i} + \mu\left[\frac{\partial \overline{U}_i}{\partial X_j}\frac{\partial \overline{U}_i}{\partial X_j} + \frac{\partial \overline{U}_j}{\partial X_i}\frac{\partial \overline{U}_j}{\partial X_j}\right]$$

If the assumption is made that

$$\frac{\rho'}{\overline{\rho}} << 1$$

the momentum equation becomes

$$\overline{\rho U}_j\frac{\partial \overline{U}_i}{\partial X_j} = \overline{F}_i - \frac{\partial \overline{P}}{\partial X_i} + \mu\frac{\partial^2 \overline{U}_i}{\partial X_j \partial X_j} + \mu\frac{\partial^2 \overline{U}_j}{\partial X_i \partial X_j} - \overline{\rho u_j\frac{\partial u_i}{\partial X_j}} \quad (A\text{-}4)$$

From the continuity equation,

$$\frac{\partial}{\partial X_j}\overline{U}_j = 0$$

Therefore, the momentum equation can be written as

$$\overline{\rho U}_j\frac{\partial \overline{U}_i}{\partial X_j} = \overline{F_i} - \frac{\partial \overline{P}}{\partial X_i} + \mu\frac{\partial^2 \overline{U_i}}{\partial X_j \partial X_j} - \overline{\rho u_j\frac{\partial u_i}{\partial X_j}} \quad (A\text{-}5)$$

If the continuity equation is multiplied by velocity, the result gives

$$\overline{\bar{U}_i \frac{\partial \bar{U}_j}{\partial X_j}} = \bar{U}_i \frac{\partial \bar{U}_j}{\partial X_j} + \overline{u_i \frac{\partial u_j}{\partial X_j}} = 0 \qquad \text{(A-6)}$$

whereby

$$u_i \frac{\partial u_j}{\partial X_j} = 0 \qquad \text{(A-7)}$$

and

$$\bar{U}_i \frac{\partial \bar{U}_j}{\partial X_j} = 0 \qquad \text{(A-8)}$$

If the term

$$- \overline{u_i \frac{\partial u_j}{\partial X_j}}$$

is added to the momentum equation, equation (A-5) becomes

$$\bar{\rho}\, \bar{U}_j \frac{\partial \bar{U}_i}{\partial X_j} = \bar{F}_i - \frac{\partial \bar{P}}{\partial X_i} + \frac{\partial}{\partial X_j}\left(\mu \frac{\partial \bar{U}_i}{\partial X_j} - \overline{\rho u_i u_j}\right) \qquad \text{(A-9)}$$

where the term $\overline{\rho u_i u_j}$ is known as the Reynolds shear stresses. Equation (A-9) is known as the turbulent momentum equation and is identical to equation (3-4) found in Chapter III.

III. Energy Equation

Turbulent flow requires a continuous supply of energy because it is of a dissipative nature. By determining the various terms of the energy equation, the amount of dissipation and production of turbulence can be found.

Primarily the derivation consists of equating the work done by the stresses to the term

$$\frac{1}{\rho} \frac{\partial}{\partial X_i} \sigma_{ij}\, U_j$$

The introduction of momentary terms and averaging with time results in the equation

$$\frac{d}{dt} \overline{\frac{q^2}{2}} = - \frac{\partial}{\partial X_i} \overline{u_i \left(\frac{P}{\rho} + \frac{q^2}{2}\right)} - \overline{u_i u_j} \frac{\partial \bar{U}_j}{\partial X_i} + \nu \frac{\partial}{\partial X_i} \overline{u_j \left(\frac{\partial u_i}{\partial X_j} + \frac{\partial u_j}{\partial X_i}\right)} - D$$

where D is defined as

$$D = -\nu\overline{\left(\frac{\partial u_i}{\partial X_j} + \frac{\partial u_j}{\partial X_i}\right)\frac{\partial u_j}{\partial X_i}}$$

The various terms of the equation are defined as:

$\frac{d}{dt}\frac{q^2}{2} \equiv$ change in kinetic energy per unit mass

$-\frac{\partial}{\partial X_i}\overline{u_i\left(\frac{P}{\rho} + \frac{q^2}{2}\right)} \equiv$ convective diffusion by turbulence

$-\overline{u_i u_j}\frac{\partial \bar{U}_j}{\partial X_i} \equiv$ energy transferred from mean motion through turbulent shear stresses

$\nu\frac{\partial}{\partial X_i}\overline{u_j\left(\frac{\partial u_i}{\partial X_j} + \frac{\partial u_j}{\partial X_i}\right)} \equiv$ work done by viscous shear stresses

$\nu\overline{\left(\frac{\partial u_i}{\partial X_j} + \frac{\partial u_j}{\partial X_i}\right)\frac{\partial u_j}{\partial X_i}} \equiv$ dissipation per unit mass by turbulent motion

If the fluid is incompressible,

$$\overline{u_j \frac{\partial^2 u_i}{\partial X_i \partial X_j}} = 0$$

The turbulence energy equation is derived in detail in Hinze (5), pages 62-69. The energy equation envolves lengthy manipulation of terms in the derivation. It is for this reason that the turbulence energy equation is not derived in detail in this appendix.

APPENDIX B: PRINCIPLE AND PROCEDURE IN TURBULENCE MEASUREMENTS

I. Principle of Hot-wire Anemometry

There are two methods in which turbulent velocities may be measured. One method is to make use of flow visualization aids such as tracers (smoke for example) and use some method of photographic recording. The second method makes use of a detecting element introduced into the flow field such that the element is sensitive enough to record small differences in turbulent fluctuations, as well as measure mean velocity. This second method is employed in the study of turbulence in the vertical atmospheric wind tunnel.

The hot-wire anemometer employs the use of a detecting element, called a probe, which consists of a thin wire, 2 to 10 microns in diameter, heated by an electric current. As the fluid passes over the wire, the wire becomes cooled, the temperature drops, and the electrical resistance of the wire decreases. The amount of heat transfer depends upon several criteria: flow velocity, temperature difference between the wire and the fluid, physical properties of the fluid, and dimensions and properties of the wire.

Neglecting heat transfer by radiation and free convection, heat transfer occurs only by conduction and forced convection. An emperical relation is derived in Hinze (5) as

$$Nu = .42Pr^{.2} + .57Pr^{.33}Re^{.5} \qquad \text{(B-1)}$$

where Nu is the Nusselt Number, Pr is the Prandtl Number, and Re is the Reynolds Number.

A film temperature T_f is defined as the average of the

wire and fluid temperature and is given by the equation

$$T_f = \frac{1}{2} (T_{wire} + T_{gas}) \qquad \text{(B-2)}$$

where the gas is considered to be the fluid in which the wire is immersed.

The heat transfer Q from the wire of the probe to the gas (ambient air) is

$$Q = a\pi ld(T_w - T_g) \qquad \text{(B-3)}$$

where a is the heat transfer coefficient, l is the length of the wire, d is the diameter of the wire, w = wire, and g = gas.

Using equation (B-1), the heat transfer becomes

$$Q = \pi k_f l(T_w - T_g)(.42Pr_f^{.2} + .57Pr_f^{.33}Re_f^{.5}) \qquad \text{(B-4)}$$

where k_f is the thermal conductivity of the film evaluated at T_f. At thermal equilibrium, the rate of heat leaving the wire must equal the heat generated by the electric current, that is

$$Q = I^2R_w \qquad \text{(B-5)}$$

where R_w is the resistance of the wire and I is the current.

Using equation (B-5), the heat transfer can therefore be written as

$$Q = I^2R_w = n\pi k_f(T_w - T_g)(.42Pr_f^{.2} + .57Pr_f^{.33}Re_f^{.5})$$

where n is defined as a conversion element since the left-hand-side of the equation above gives joules per second while the right-hand-side is in calories per second; for air, n is equal to 4.2 joules/calorie.

The right-hand-side of the equation appears as a function of T_f, which gives rise to effects of second order. The resistance of the wire gives effects of first order to the temperature. Writing the resistance of the wire as a function of temperature and expanding in a Taylor's series gives

$$R_{wire} = R_{ref.temp.}(1. + C(T_w - T_{g_o}) + C_1(T_w - T_{g_o})^2 + \cdot\cdot\cdot\cdot) \qquad (B\text{-}6)$$

where T_{g_o} is the temperature of the gas at a reference state and C and C_1 are temperature foefficients of the electric resistivity of the wire. Neglecting terms of second order (also C_1 is smaller that C):

$$R_w = R_{g_o}(1. + C(T_w - T_{g_o})$$

or

$$T_w - T_{g_o} = \frac{R_w - R_{g_o}}{CR_{g_o}} \qquad (B\text{-}7)$$

Now let

$$T_w - T_g = \frac{R_w - R_g}{CR_g} \qquad (B\text{-}8)$$

where $R_{g_o} = R_g$. The heat transfer can therefore be written as

$$I^2R_w = \frac{n\pi[k_f]1}{C}\left(\frac{R_w - R_g}{R_g}\right)(.42Pr_f^{.2} + .57Pr_f^{.33}Re_f^{.5}) \qquad (B\text{-}9)$$

or, in more convenient terms,

$$\frac{I^2R_w}{R_w - R_g} = A + BU^{.5} \qquad (B\text{-}10)$$

where

$$A = .42\left(\frac{n\pi k_f 1}{CR_g}\right)Pr_f^{.2} \qquad (B\text{-}11)$$

and

$$B = .57\left(\frac{n\pi k_f l}{CR_g}\right)Pr_f^{.33}\left(\frac{\rho D}{\nu}\right)^{.5} \qquad \text{(B-12)}$$

where ρ is the density of the fluid, D is the diameter of the wire, and ν is the kinematic viscosity of the fluid.

It is these factors, A and B, which must be determined in order to estimate the effects of the gas and wire properties. A and B are found experimentally.

For the DISA 55D01 Constant Temperature Anemometer, the equation (B-10) assumes the form

$$V^2 = V_o^2 + BU^{.5} \qquad \text{(B-13)}$$

where V is the bridge voltage and V_o is the bridge voltage at zero flow (this is explained in Chapter IV). By plotting output voltage versus velocity, a calibration curve can be made, as shown in Figure B-1. Note that the calibration of the probe must occur where there is little or no turbulence (very laminar flow).

Primarily, equipment used in these experiments consist of 2 constant temperature anemometer units, 2 linearizers, 2 digital voltmeters, 2 root-mean-square voltmeters, 1 auxiliary unit, and 2 correlators. The specific schematics for determining the various flow components of turbulence are shown in Figures B-2 and B-3.

A. Measurements with the Single Probe

The single probe consists of a DISA type 55A25 minature probe mounted in a 14 inch probe holder, bent upon request at 90^o two inches from the point where the probe is connected to the probe holder. The probe holder, permanently mounted

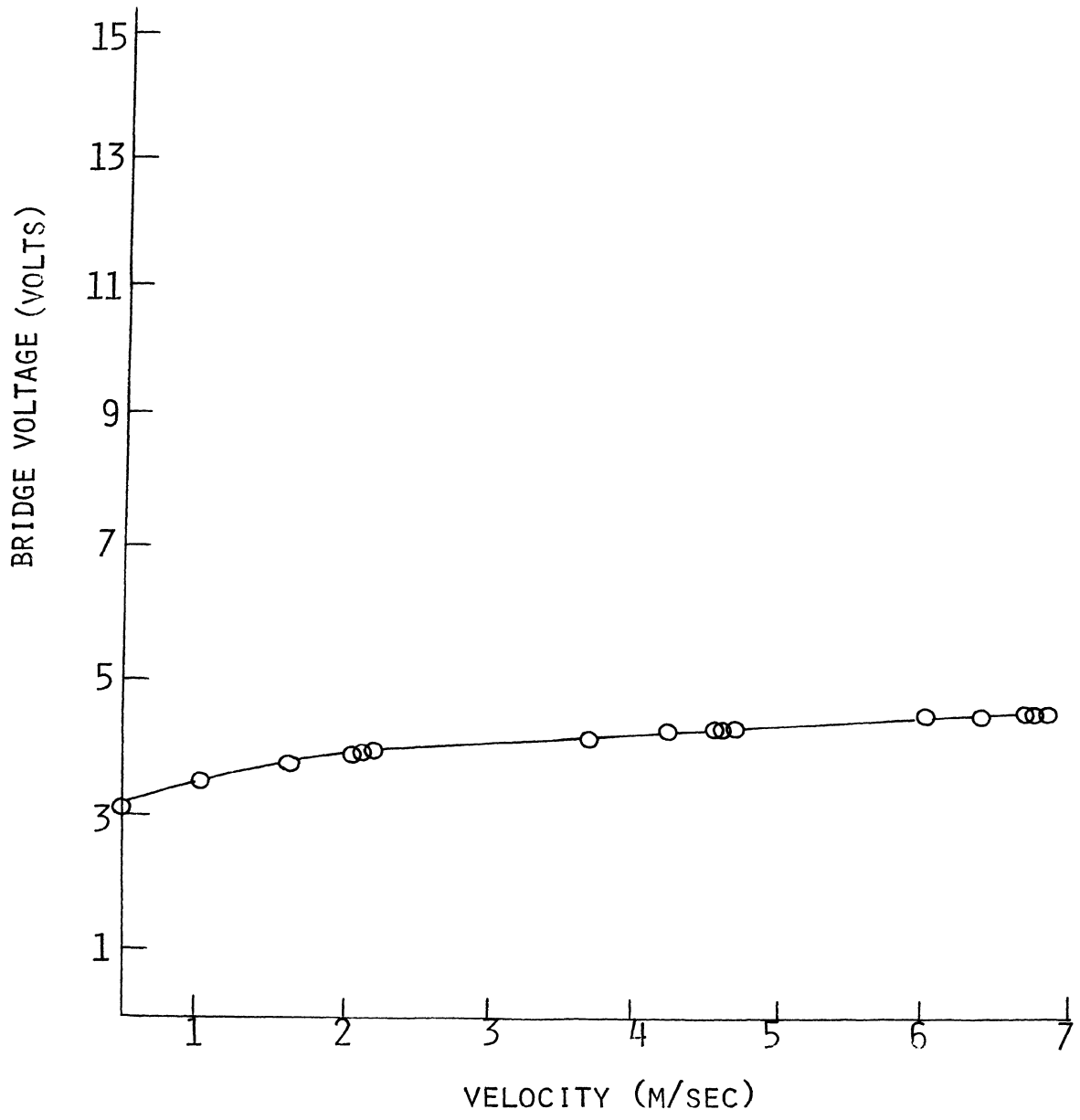

Figure B-1. Calibration Curve for DISA Type 55A25 Minature Single-wire Probe with System Non-linearized

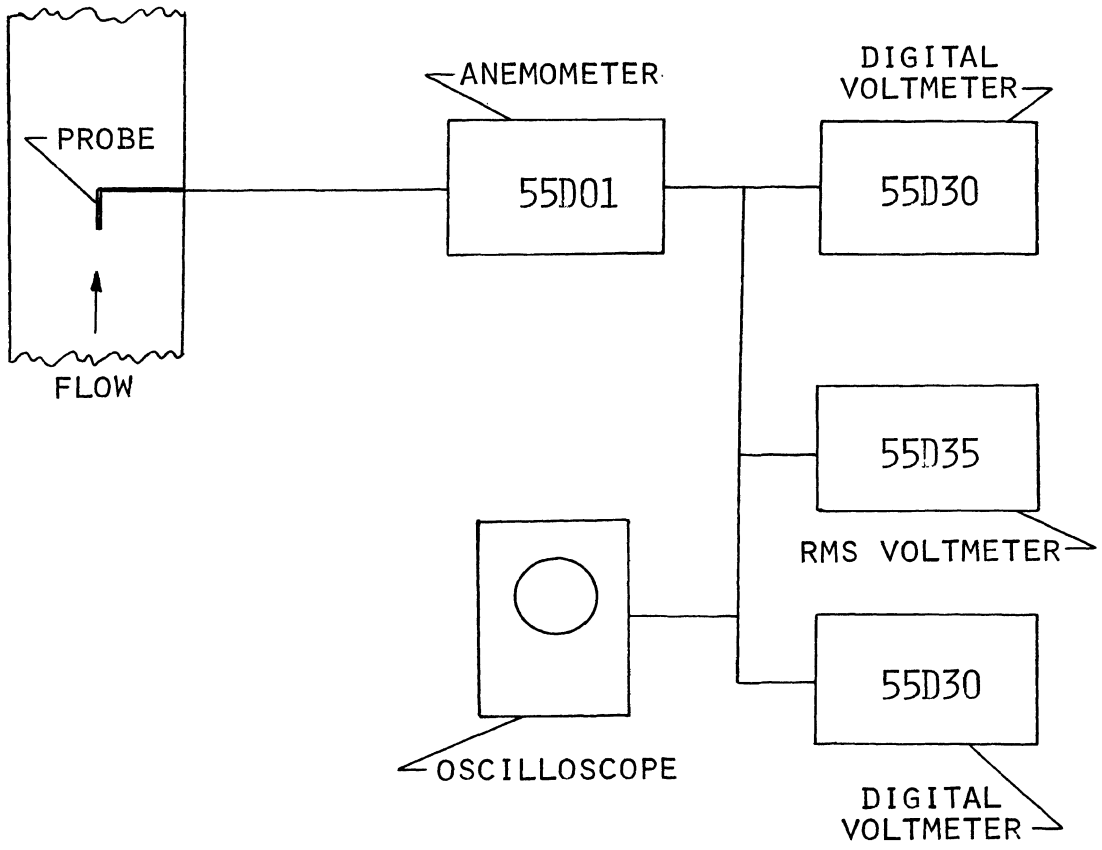

Figure B-2. Schematic for Using a DISA Type 55D01 CTA Unit with a Single-wire Probe

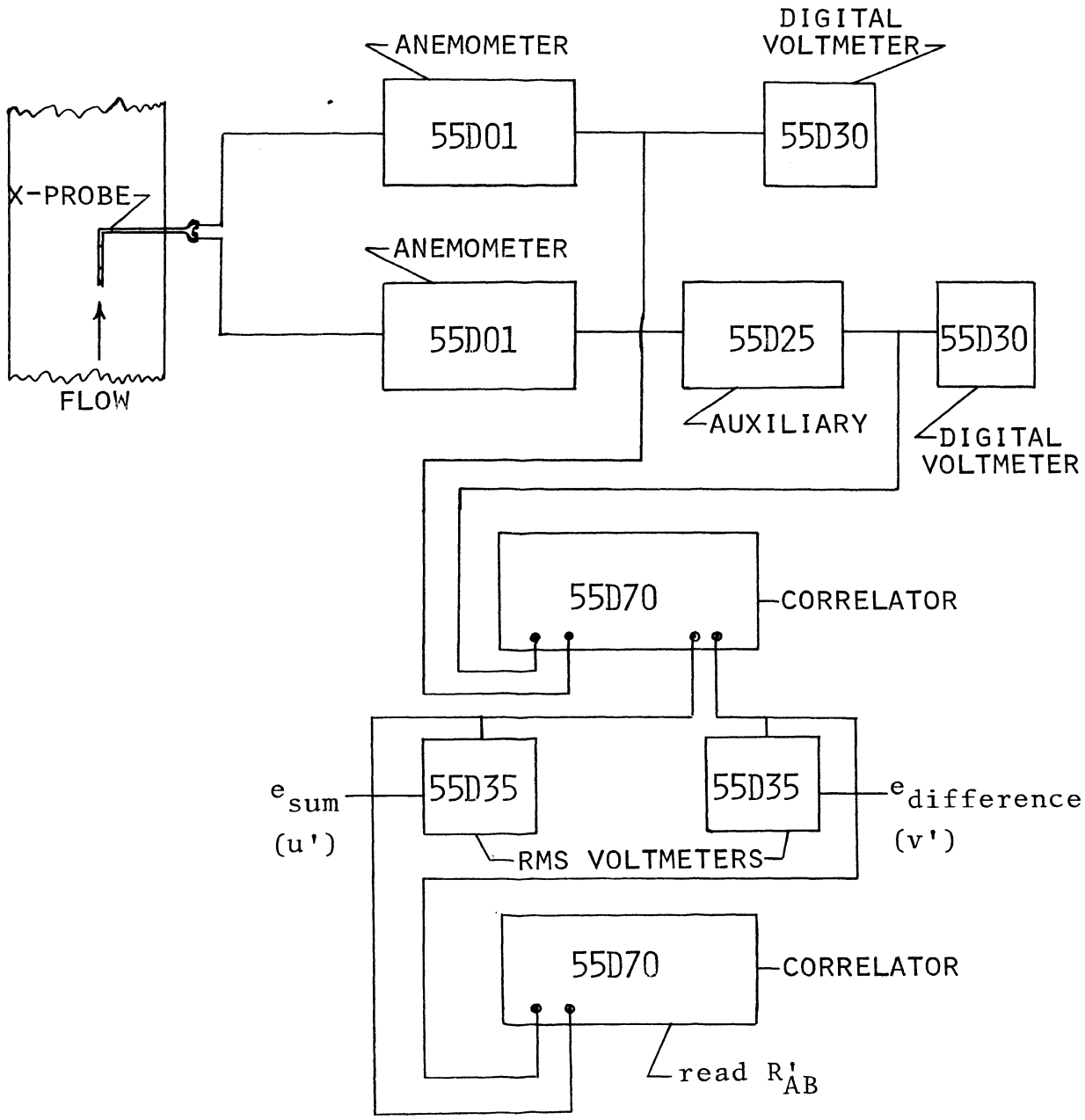

Figure B-3. Schematic for Using a DISA Type 55D01 CTA Unit with an X-wire Probe

in a circular piece of plexiglass, is introduced into the wind tunnel with the minature probe attached such that the hot-wire is always 90^{o} to the direction of flow (refer to Figure 8). In this configuration, the mean velocity profiles of both the test section and the wake of the sphere can be measured along with the longitudinal turbulent intensities for each case. The readings of both the mean velocity voltage and turbulent component voltage are read directly from the digital voltmeter and root-mean-square voltmeter respectively and can be programmed into a Wang Computer to give u' and U .

B. Measurements with the X-probe

The X-probe consists of a DISA type 55A32 X-probe mounted on a DISA probe holder approximately 6 inches long with a 90^{o} adaptor attached. The X-probe and holder are mounted in a circular piece of plexiglass, similar to the single probe mounting, and introduced into the test section at varying positions from the inlet of the test section.

Each wire is connected to a 55D01 CTA and the output bridge voltages equalized by introducing an auxiliary unit 55D25 (variable gain device) into the unit with the lower output. By adjusting the gain of the auxiliary unit until both digital voltmeters read the same value, the systems can frequently be equalized and the sensitivities of the wires made equal.

The two equalized signals are fed into a 55D70 Correlator and the sum and difference of the two signals recorded on root-mean-square voltmeters and the u_z' and u_r' values deter-

mined by using an IBM 360/50 Digital Computer. Rotating the probe 90^{o} gives u'_z and u'_θ. Correlating the sum and difference signals, where signals from the sum and difference outputs of the first correlator are fed into a second correlator, gives the cross-correlation factor R'_{AB}, which is a function of the shear stresses.

II. General Procedure in Using the DISA Anemometer System

A. Type 55D01 Anemometer Unit

1. Connecting instrument to power supply

   a. check voltage displayed in window on back of unit

   b. if voltage must be changed (220 - 110V)

      i. remove 4 screws and take off rear panel

      ii. pull out switch plug behind windows, turn it, and re-insert so that desired legend appears

      iii. replace fuse with slow-blow fuse (if using 110V) and replace spare fuse at power socket

      iv. put rear panel on

   c. set loop control (front panel on standby

   d. connect line voltage to power line socket

   e. turn switch (rear panel) on

   f. turn meter switch all the way to the left and check that the meter reads approximately 3/4 full scale deflection

2. Using normal probes in air flow measurements

   a. connect instrument to power line. Check line voltage (meter switch) and wait several minutes

   b. turn meter switch to current adj. line

   c. adjust current adj. control screw for meter reading of 3.5 ma (top scale)

   d. turn meter switch to 30.0

   e. turn gain adj. screw to 1 (fully left)

f. set resistance-o-temp. switch to neutral

g. connect 5 meter cable to probe terminal, connect probe support to other end of 5 meter cable, and short probe support with either piece of wire stuck in the end of the support or with a shorting probe

h. set LF gain switch at flat

i. put screw driver into output bias slot and adjust the screw until needle of meter is approximately centered on scale (5 on top scale)

j. adjust HF filter so that it is set at 1

k. cable compensation Q and L: temporarily adjust these screws until they are approximately 1 mm from the front surface of the panel

l. cable compensation, zero ohms:

i. type 9006A1864 5-meter probe cable is connected to terminal (should already be done) with probe support shorted

ii. set probe resistance ohms switches to 0

iii. set meter switch to 30

iv. bridge ratio switch set at 1:20

v. LF gain switch turned to high

vi. adjust input bias control until needle is centered on scale (5 on top scale)

vii. depress resistance-o-temp. switch. If needle deflects, adjust zero ohms control with screwdriver until needle no longer deflects when resistance-o-temp. switch is depressed

viii. resistance in cable has now been compensated

3. Probe turn on procedure

a. check the following steps

i. turn meter switch to 10

ii. set loop control at standby

iii. set bridge ratio at 1:20

iv. LF gain at high

b. disconnect the wire from the probe support and put the probe into the probe holder, making sure that the probe slips onto the protrusion in the middle of the probe support

c. depress resistance-o-temp. switch. Needle will now deflect

d. adjust the probe resistance ohms decades until the needle no longer deflects when the resistance-o-temp. switch is depressed

e. probe resistance now equals the value in the windows. Set gain adj. to 3 and HF filter to 2. Note: if this cannot be accomplished or if the input bias cannot be adjusted for half scale meter deflection, the probe is broken

f. set decade resistance at a value of 1.a times the probe resistance, where a = .8 for air and is known as the overheat ratio.

g. turn loop control to internal. Anemometer servo loop is closed and probe will heat up. Anemometer is now in operation

B. Type 55D25 Auxiliary Unit

1. Connecting instrument to power supply

a. make sure voltage selector on rear panel of instrument is set for local power line

b. connect power cable and switch on instrument

2. Square wave generator

a. connect 06A186 1-meter cable from square wave output terminal to the test in terminal on rear panel of 55D01 anemometer unit

b. set frequency switch to desired range, normally at 3kHz

c. set amplitude control for approximately 0.5 volts peak to peak output test signal from anemometer. Note:

i. anemometer must be in operation, i.e., loop control must be turned to int.

ii. connect 06A186 1-meter cable from amplifier out terminal of anemometer to positive terminal of oscilloscope and visually adjust amplitude control of auxiliary square wave unit until 0.5 V peak to peak is obtained

d. turn frequency switch on auxiliary unit (Square Wave Generator) to 3kHz, making sure that the loop control of the anemometer is at int.

e. expose probe to maximum velocity and stepwise increase the gain adj. control while simultaneously adjusting controls Q and L until stability is obtained at maximum possible gain

f. adjust the L control at different settings of Q until the best possible square wave test curve appears. Do not advance the Q control more than necessary to suppress oscillation

g. switch off square wave generator after adjusting oscillation

3. Using the amplifier

a. connect amplifier out terminal of anemometer to input terminal of auxiliary with a 06A186 1-meter cable

b. connect recording instruments (DISA type 55D35 and digital DC voltmeter) to output terminals

c. set filters for desired upper-frequency and lower-frequency limits

d. set gain control for desired gain level

e. set zero adj. control for zero DC output for either no flow or flow on the probe, depending on where the DC component of bridge voltage is undesirable

C. Type 55D35 RMS Voltmeter

The 55D35 RMS voltmeter is designed for measurement of the actual root-mean-square value of AC voltages between 300 volts and 300 volts rms.

1. Turn on procedure

a. check line voltage as was done for anemometer and auxiliary units on rear panel

b. power is applied by turning power switch on

c. let unit warm up for 1/2 hour.

d. attach test lead to input terminal

2. Operating instructions

a. set range switch to 300 volts

b. connect test lead to point to be measured

c. rotate range switch in a counter clock-wise direction until direct reading meter shows reading in the upper two-thirds of the scale

d. set integrator time constant switch for best possible response time, depending on the waveform and frequency of the voltage under measurement

D. Type 55D10 Linearizer

The 55D10 linearizer is basically an electronic analog computer. The linearized output voltage is proportional to the velocity whereby

$$V_{out} = k(A + BU^{.5} - V_{in}^2)^m$$

where k is a constant found from a calibration curve (see Figure B-1) and m is an exponential constant (see below).

1. Connecting the instrument to the power line

   a. check the rear wall of the linearizer for line voltage and fuse rating, indicated by the line voltage selector

   b. apply line power to power recepticle on rear wall and depress on/off push button switch

2. Connecting the instrument to a 55D01 anemometer

   a. set the mode selector to 2 and adjust the exponent m with the exponent control

   b. set the range switch to 4

   c. at zero velocity, reduce the operating resistance, corresponding to the decade resistance setting on the anemometer, until the anemometer output voltage reaches the value V_{o_1} where

$$V_{o_1} = .925\ V_o$$

   d. connect anemometer bridge top output to the linearizer input

   e. press zero pushbutton and adjust the two zero adj. controls for zero output voltage from the linearizer

f. release the zero pushbutton and set the resistance decades to their initial value of operating resistance

g. press the temp. compensation pushbutton and adjust the temperature compensation control for zero output voltage from the linearizer

h. release the temp. compensation pushbutton

i. adjust the level control for zero voltage at the output connector with the X1 - X10 pushbutton in the X10 position and with no voltage applied through the input connector

j. adjust the calibration equipment to give the velocity U

k. adjust the two gain adj. controls so that a linearizer output voltage is obtained that shows some simple relation to the velocity. At maximum velocity, the voltage should be $\leq$ 10 volts. The linearization accomplished by these adjustments will in general be adequate for most turbulence measurements

E. Type 55D70 Analog Correlator

The DISA Analog Correlator measures the cross-correlation coefficient and the cross-correlation factor of two signals (with an external time delay inserted into one channel both auto- and cross-correlation functions can be measured).

1. Operating instructions

a. to turn on power

i. zero the direct reading meter with screw driver control (set zero)

ii. check line voltage on back of correlator to correspond with correct line voltage

iii. set measurement function switch in R position

iv. plug line outlet from correlator into input socket of power source

v. set power switch on rear of panel to <u>on</u> position

vi. allow unit to warm up for 1/2 hour

b. measurement of the cross-correlation coefficient

i. set range volt switches to 10 volts

ii. turn variable gain controls fully counter clock-wise

iii. connect cables from source to be correlated to input A and input B

iv. to normalize the signal A:

1.) set measurement function switch to the $\overline{e_A^2}$ position

2.) turn integration time constant switch to 0.1 sec

3.) turn range volts switch counter clock-wise until the meter reads between the red mark and 0.1 on the upper right scale

4.) adjust the time constant so that the needle does not deflect

5.) turn the gain control clock-wise until the meter deflects to the red mark

v. to normalize the signal B:

1.) set measurement function switch to the $\overline{e_B^2}$ position

2.) turn integration time constant switch to 0.1 sec

3.) turn range volts switch counter clock-wise until the meter reads between the red mark and 0.1 on the upper right scale

4.) adjust the time constant so that the needle does not deflect

5.) turn the gain control clock-wise until the meter deflects to the red mark

vi. to measure the cross-correlation coefficient ρ_{AB}

1.) set measurement function switch to the correlation coefficient range providing the greatest possible meter sensitivity

2.) select the time constant so that the meter deflection does not fluctuate

3.) the cross-correlation coefficient ρ_{AB} may be read on the meter scale corresponding to the settings of the measurement function switch

4.) voltage is proportional to ρ_{AB} at the correlation function output

c. measurement of the cross-correlation factor R_{AB}

i. set the range volts switches to 10 volts and turn the variable gain controls fully clock-wise to the cal. position

ii. apply signals to be correlated through input A and input B

iii. to set range of measurement for channel A

1.) set measurement function switch to $\overline{e_A^2}$

2.) set integrating time constant switch to 0.1 sec

3.) turn range volts switch in a counter clockwise direction until the meter reads between the red mark and 0.1 on the upper right scale

4.) select the time constant so that the meter deflection does not fluctuate

iv. to set range of measurement for channel B

1.) set measurement function switch to $\overline{e_B^2}$ position

2.) set integrating time constant switch to 0.1 sec

3.) turn range volts switch in a counter clockwise direction until the meter reads between the red mark and 0.1 on the upper right scale

4.) select the time constant so that the meter deflection does not fluctuate

v. to measure the cross-correlation factor R_{AB}

1.) turn measurement function switch to the correlation factor R

2.) set the time constant switch so that the meter deflection does not fluctuate

3.) upper scale meter reading, R'_{AB} in volts square, is proportional to the value R_{AB} such that

$$R_{AB} = R'_{AB}\ G_A\ G_B$$

(a) G_A and G_B are settings of range volts switches for channels A and B

(b) since range volts attneuators are calibrated in steps of 10 db, the 3×10^n position is replaced by 10×10^n (n = -3, -2, -1, 0)

4.) a voltage proportional to R'_{AB} is available at the correlation function output terminal

2. Measuring correlation functions

   a. must employ a time delay unit

   b. can measure auto-correlation and cross-correlation functions (see DISA Techanical Notes)

3. Measuring spatial correlation coefficients

   a. g(r) and f(r)

   b. see DISA manual Type 55D70 Analog Correlator

4. Measuring Macro and Micro scales of turbulence

   a. see DISA manual Type 55D70 Analog Correlator

5. Measuring auto-correlations

   a. see DISA manual Type 55D70 Analog Correlator

6. Measuring Reynolds shear stress

   a. this is a correlation between u' and v' and u' and w' turbulent velocities

   b. calculate R'_{AB}

   c. refer to Chapter IV, equation (4-21)

   d. refer to Figure B-3

7. Triple correlation measurements

   a. k(r,t), h(r,t), and q(r,t)

   b. connect signal e_A to input of 55D35 RMS voltmeter and turn range switch to a meter deflection of 1/3

c. on squared signal output an instantaneous voltage e_{sq} is available such that

$$e_{sq} = K \left(\frac{e_{in}}{G} \right)^2$$

$$e_A^2 = e_{in}^2 = \frac{G}{K} e_{sq}$$

where G is the position of the range switch and $K = 1/2$ volt^{-1}

d. connect the squared signal e_{sq} to the input A and the signal e_B to the input B on the correlator

e. operate the correlator as described in the operating instructions

f. the triple correlation is given by

$$R_{AB} = G_A G_B R'_{AB} = \overline{e_{sq} e_B}$$

$$R_{AB} = \frac{K}{G^2} \overline{e_A^2 e_B}$$

$$e_A^2 e_B = \frac{G_A G_B G^2}{K} R'_{AB} = 2 G_A G_B G^2 R'_{AB}$$

$$K(r,t) = \frac{e_A^2 e_B}{e'^3}$$

where e' is the root-mean-square value of e_A or e_B.

III. Simplified Operating Instructions for Using the DISA 55D01 Anemometer

A. 55D01 in a Constant-current Mode for Large Temperature Fluctuations

1. turn instrument on and allow sufficient warm up time
2. measure resistance in the normal manner, steps one through three for the CTA mode, and leave decades in position
3. set LF response at flat

4. set gain adj. to 9

5. switch loop control to Ext.

6. set temperature-o-resistance switch to temperature

7. readout is from amplifier output jack

8. with input bias set at midscale, output at ambient conditions will be 15 volts

9. measurements can now be made when temperature is varied by taking the voltage difference and reading the temperature off a calibration curve

10. if an auxiliary unit (55D25) or a Linearizer 55D10 is available, the initial 15 volts can be suppressed and voltages read more accurately

B. 55D01 in the Constant Temperature Mode for Small Temperature Fluctuations

1. turn instrument on and allow sufficient time to warm up

2. measure resistance in the normal manner, steps one through three for the CTA mode

3. multiply the resistance by 1.02 and set decades at this value

4. set LF response to flat

5. turn loop control to int. and note bridge voltage

6. this bridge voltage is the reading for ambient temperature

7. the voltage difference from this voltage is proportional to the temperature change and is read off a calibration curve

C. 55D01 in the Constant Temperature Mode with a Film Probe in Air

1. turn instrument on and allow sufficient warm up time

2. set controls as follows:

   a. meter switch to 1, 3, 10, or 30
   b. decade resistance to 00.00
   c. loop control at Stby.
   d. bridge ratio at 1:20
   e. HF filter at 1

f. gain adj. at 4
g. LF response at high
h. temperature-o-resistance switch at neutral

3. connect 5-meter probe cable with probe support and shorting probe to probe jack. Set input bias at half scale deflection

4. adjust the zero ohms with a screw-driver so that there is no meter deflection when the temperature-o-resistance switch is depressed

5. replace the shorting probe with the actual probe. Set decade resistance to a value that gives no meter deflection when the temperature-o-resistance switch is depressed

6. probe should be in the medium it will be used in when the resistance is taken

7. note the resistance on the decade box and multiply this value by 1.6. Set this result on the decade box.

8. turn to int. on loop control to operate

D. 55D01 in the Constant Temperature Mode with a Film Probe in Water

1. - 5. same procedure as for film probe in air

6. note resistance on decade box and multiply this value by 1.1. Set this result on the decade box.

7. turn to int. on the loop control to operate

APPENDIX C. INSTRUMENT CALIBRATION

I. Single Wire

The DISA type 55A25 minature probe was used in conjunction with the DISA CTA, auxiliary unit, root-mean-square voltmeter, and digital voltmeter. Since the single probe calibrated more closely to the pitot-static probe measurements than the X-probe, the single probe measurements were taken as being the most accurate. Equation (4-4) was used where only bridge voltage, the root-mean-square value of the bridge voltage, and known mean velocity (from pitot-static probe measurements) were recorded, then fed into the Wang computer. Table C-1 shows a tabulation of the longitudinal intensity, u'/U , for the single probe as compared with the longitudinal intensity measured with an X-probe.

II. X-wire Cross-correlation Coefficient Method

With reference to Chapter IV, values of velocity normal to the X-wires were recorded for the xz plane such that the X-wires would give simultaneous values for u' and v'. v' proved to be half the value of u'. However, since the single wire measures only the u' component of velocity, the longitudinal turbulence intensity of the X-probe is the only value recorded and is tabulated in Table C-2.

The equation

$$\frac{\sqrt{\overline{q_A^2}}}{U_{eff}} = \frac{4}{1 - \left(\frac{V_o}{V_A}\right)^2} \frac{\sqrt{\overline{e_A^2}}}{V_A} \qquad \text{(C-1)}$$

TABLE C-1

A comparison of methods for measuring Longitudinal Turbulence

position from left wall	single wire method	cross-corr. method	sum-diff. method
y	$\frac{u'}{U}$	$\frac{u'}{U}$	$\frac{u'}{U}$
.25	.091	.104	.113
.50	.035	.033	.035
.75	.048	.052	.049

TABLE C-2

Calibration of X-probe with single-wire probe

		1-fan			3-fans		
		X-probe		single	X-probe		single
z	y	$\frac{u'}{U}$	$\frac{v'}{U}$	$\frac{u'}{U}$	$\frac{u'}{U}$	$\frac{v'}{U}$	$\frac{u'}{U}$
42.6"	.5"	.0515	.0310	.0595	.0438	.0212	.0433
"	1.0	.0059	.0043	.0067	.0053	.0026	.0051
"	1.5	.0042	.0023	.0047	.0049	.0019	.0047
"	2.0	.0042	.0021	.0045	.0048	.0018	.0044
"	2.5	.0045	.0020	.0043	.0049	.0017	.0041
"	3.0	.0040	.0020	.0043	.0046	.0017	.0043
"	3.5	.0043	.0021	.0041	.0045	.0017	.0043
"	4.0	.0052	.0023	.0045	.0049	.0019	.0041
"	4.5	.0065	.0038	.0052	.0051	.0025	.0048
"	5.0	.0257	.0133	.0248	.0247	.0157	.0241
"	5.5	.0946	.0596	.0953	.0945	.0605	.0927

holds for any hot-wire normal to the direction of flow, i.e., 90^{o} with respect to the wire's length. If the wires of the X-probe are mutually 45^{o} to the direction of flow, the component of velocity in the direction of the flow can be written as

$$u = .707\ (q_{A_{xz}} + q_{B_{xz}}) \tag{C-2}$$

where A and B denote the wires A and B, respectively.

Squaring both sides and time averaging gives

$$\overline{u^2} = .5\ \overline{(q_{A_{xz}} + q_{B_{xz}})^2} \tag{C-3}$$

or

$$\overline{u^2} = .5\ (\overline{q^2_{A_{xz}} + q^2_{B_{xz}}}) + \overline{q_{A_{xz}} q_{B_{xz}}} \tag{C-4}$$

The anemometer cannot measure the value $\overline{q_{A_{xz}} q_{B_{xz}}}$. To eliminate this problem, the cross-correlation coefficient, ρ_{AB}, is introduced whereby

$$\rho_{AB} = \frac{\overline{q_{A_{xz}} q_{B_{xz}}}}{\sqrt{\overline{q^2_{A_{xz}}}}\sqrt{\overline{q^2_{B_{xz}}}}} \tag{C-5}$$

Taking the square root of both sides of equation (C-4),

$$\sqrt{\overline{u^2}} = \left[.5\ (\overline{q^2_{A_{xz}} + q^2_{B_{xz}}}) + \overline{q_{A_{xz}} q_{B_{xz}}}\right]^{.5} \tag{C-6}$$

and introducing equations (C-1) and (C-5) into equation (C-6) results in

$$\sqrt{\overline{u^2}} = \left\{ .5\left[\left(\frac{4\ U_{eff}}{1 - \left(\frac{V_o}{V_A}\right)^2}\ \frac{1}{V_A}\right)^2 \overline{e_A^2} + \left(\frac{4\ U_{eff}}{1 - \left(\frac{V_o}{V_B}\right)^2}\ \frac{1}{V_B}\right)^2 \overline{e_B^2}\right] + \rho_{AB}\sqrt{\overline{q^2_{A_{xz}}}}\sqrt{\overline{q^2_{B_{xz}}}} \right\} \tag{C-7}$$

where $q^2_{A_{xz}}$ and $q^2_{B_{xz}}$ are defined in equation (C-1).

Equalizing both bridge voltages (using either an auxiliary unit or a Linearizer) whereby $V_A = V_B$, equation (C-7) becomes

$$\sqrt{\overline{u^2}} = \frac{4\ U_{eff}}{1 - \left(\frac{V_o}{V_B}\right)^2} \frac{1}{V_B} \left[\frac{1}{2} \left(\overline{e^2_{A_{xz}}} + \overline{e^2_{B_{xz}}} \right) + \rho_{AB} \sqrt{\overline{e^2_{A_{xz}}}} \sqrt{\overline{e^2_{B_{xz}}}} \right]^{.5}$$

where

$$U_{eff} = U \frac{\sqrt{2}}{2}$$

The equation for u'/U can therefore be written as

$$\frac{u'}{U} = \frac{2.82}{1 - \left(\frac{V_o}{V_B}\right)^2} \frac{1}{V_B} \left[\frac{1}{2} \left(\overline{e^2_{A_{xz}}} + \overline{e^2_{B_{xz}}} \right) + \rho_{AB} \sqrt{\overline{e^2_{A_{xz}}}} \sqrt{\overline{e^2_{B_{xz}}}} \right]^{.5} \quad \text{(C-8)}$$

The turbulence intensity in the y direction (v'/U) is written as

$$\frac{v'}{U} = \frac{2.82}{1 - \left(\frac{V_o}{V_B}\right)^2} \frac{1}{V_B} \left[\frac{1}{2} \left(\overline{e^2_{A_{xz}}} + \overline{e^2_{B_{xz}}} \right) - \rho_{AB} \sqrt{\overline{e^2_{A_{xz}}}} \sqrt{\overline{e^2_{B_{xz}}}} \right]^{.5} \quad \text{(C-9)}$$

where ρ_{AB} is the cross-correlation coefficient as used throughout the above equations.

III. X-wire Sum-Difference Technique

The sum and difference of the two quantities, $e_{A_{xz}}$ and $e_{B_{xz}}$, can easily be found by using the 55D70 Correlator and two root-mean-square voltmeters (DISA 55D35 RMS Voltmeter).

The procedure is identical as for the cross-correlation coefficient method except that the cross-correlation coefficient does not have to be found. In using the DISA Correlator, the signals from both anemometers (e_A and e_B) have to first be

attenuated using the Range Volts controls on the Correlator, then the Gain Adjustments (both A and B signals) turned to the Cal. position to ensure that both signals have equal gain. Equation (C-8) reduces to

$$\frac{u'}{U} = \frac{.707}{2s}\sqrt{\overline{(e_{A_{xz}} + e_{B_{xz}})^2}} \qquad \text{(C-10)}$$

where s is the sensitivity factor as defined in Chapter IV.

APPENDIX D: DATA REDUCTION TECHNIQUES

I. The Wang 370 Computer System

The Wang 370 Computer System consists of three fundamental units: the Arithmetic Calculator, the 370 Keyboard Programmer, and a cassette tape reader. The Arithmetic Calculator performs basic arithmetic operations, the Keyboard Programmer provides a keyboard for data entry and display and sequencing logic for card reader programs, and a data storage unit stores data and an input/output unit provides automatic output of data (Model 379-5/7 Output Writer). The Output Writer is an IBM Selectric typewriter with a slight modification (refer to "Iterim Instruction Manual Model 379-5/7 Output Writer---Operating Instructions"). Magnetic tapes with storage up to 640 steps (operations) are put into the rear of the Keyboard and the programs stored onto the magnetic tapes by pressing the keys. A tape drive within the Calculator controls the Selectric typewriter (read/write unit) output.

A. Pressure-Velocity Program

The pressure in mm Hg is recorded using an MKS Baratron Electronic Pressure Meter and the values punched directly into the computer, giving velocity in ft/sec as well as m/sec. This program prints out pressure in mm Hg, velocity in m/sec, and velocity in ft/sec, respectively, in three distinct columns. The program is written as follows:

```
07 - mark
60 - zero
17 - recall full
61 - store value of pressure
24 - write
71 - store
24 - write
```

```
23 - special format
44 - square root
41 - enter
63 - 3
75 - decimal point
66 - 6
63 - 3
67 - 7
66 - 6
60 - 0
67 - 7
65 - 5
46 - multiply
41 - enter
17 - recall full
67 - 7
46 - multiply
24 - write
23 - special format
01 - stop
```

The procedure in running the program is as follows:

1. record the value of $\sqrt{T/\rho}$ on the numeric keys of the Keyboard, where T is the mean temperature and ρ is the mean density of air. Make sure the tape button is pushed to the "learn" position.
2. press the store-full key
3. press key 67 (small numbers) and put the tape button on the "run" position
4. record the value of the meter reading for pressure on the numeric keys
5. press the store-full key
6. press key 61
7. press the clear-all key
8. press the search key
9. press key 60 (small numbers) and read the velocity on the typewriter output
10. repeat procedures 4 through 9 for new value of pressure

B. Relative Turbulence Intensity Program

The mean velocity, in m/sec, the bridge voltages at both zero flow and flow conditions, and the root-mean-square values of the bridge voltages at various velocities are fed into the Wang Computer (refer to equation (4-4)). The output gives the u' component of flow, the mean velocity U , and the turbulence intensity u'/U in respective columns. The program is written as follows:

07 - mark
60 - zero
24 - write
71 - store 9
17 - recall full
61 - store value of $\sqrt{\overline{v^2}}$
41 - enter
17 - recall full
62 - store V (bridge voltage)
47 - divide
13 - store full
66 - store value $\sqrt{\overline{v^2}}/V$
61 - store value of the quantity $\sqrt{\overline{v^2}}$
41 - enter
17 - recall full
62 - store V
47 - divide
45 - square
41 - enter
17 - recall full
63 - enter the value V_o^2
46 - multiply
13 - store full
67 - enter the value $\left(V_o/V\right)^2$
50 - clear adder
77 - change sign
52 - add
61 - enter the value $\sqrt{\overline{v^2}}$
75 - decimal point
52 - add
13 - store full
65 - enter the value $1 - \left(V_o/V\right)^2$
64 - enter 4
75 - decimal point
41 - enter
17 - recall full
65 - enter the value $1 - \left(V_o/V\right)^2$
47 - divide
41 - enter
17 - recall full

66 - enter the value $\sqrt{v^2}$ /V
46 - multiply
24 - write
23 - special format
41 - enter
17 - recall full
70 - enter mean velocity
24 - write
76 - clear display
24 - write
23 - special format
46 - multiply
24 - write
76 - clear display
24 - write
23 - special format
01 - stop

The procedure in running the program is as follows:

1. for the initial run:
   a. push switch to "run" (tape removed from "learn" position
   b. enter V_o^2 into number 63 key (small numbers)
2. enter $\sqrt{v^2}$ into key 61 (small numbers)
3. enter V (bridge voltage) into key 62 (small numbers)
4. enter U in key 70 (small numbers)
5. push clear-all key
6. set typewriter tabs for 3 print-out answers
7. push search key
8. press key 60
9. repeat steps 2 through 9 for new values of $\sqrt{v^2}$, V, and U .

Note: Before the program is entered onto the tape, i.e., the specific keys punched to program the tape, the following procedure should be done to ensure no additional data is on the tape in use:

1. insert tape in rear of Keyboard
2. push switch to learn position

3. push clear-all key

4. push erase key (red light will come on showing that the tape is running and will shut off when the tape is fully erased)

5. punch program

II. The IBM 360/50 Digital Computer Program

The IBM 360/50 Digital Computer is used to calculate turbulence intensities and Reynolds shear stresses for data recorded by a DISA 55A32 X-probe. Values of voltage are recorded and reduced to specific turbulence values using the equations derived in Chapter IV. The computer program is written as follows:

```
C
C      PROGRAM WHICH CALCULATES U', V', W', U'V', AND U'W' FROM
C      KNOWN VALUES MEASURED WITH A DISA 55D01 CTA
C      DIAMETER OF SPHERE = 1.25"
C
       DIMENSION V(7,2,22),X(22),Y(7),F(2),RABV(7,2,22),GAV(7,2
      $,22),GBV(7,2,22),RABW(7,2,22),GBW(7,2,22),GAW(7,2,22),ES
      $V(7,2,22),EDV(7,2,22),EDWV(7,2,22),UP(7,2,22),VP(7,2,22)
      $,WP(7,2,22),S(7,2,22),UPVP(7,2,22),UPWP(7,2,22)
       X(1)=1.
       DO 1 I=2,22
     1 X(I)=X(I-1)+1.
       READ,(Y(K),K=1,7)
       F(1)=1.
       F(2)=2.
       VO=6.08
C      READ VALUES RECORDED BY DISA 55D01 CTA
C
       DO 3 K=1,7
       DO 3 J=1,2
       READ,(V(K,J,I),I=1,22)
       READ,(ESV(K,J,I),I=1,22)
       READ,(EDV(K,J,I),I=1,22)
       READ,(EDWV(K,J,I),I=1,22)
       READ,(RABV(K,J,I),I=1,22)
       READ,(GAV(K,J,I),I=1,22)
       READ,(GBV(K,J,I),I=1,22)
       READ,(RABW(K,J,I),I=1,22)
       READ,(GAW(K,J,I),I=1,22)
       READ,(GBW(K,J,I),I=1,22)
     3 CONTINUE
C
C      CALCULATE U',V',W' WHEREBY U' = SQRT(UBAR**2)/UO, ETC.
C
```

```
      DO 4 K=1,7
      DO 4 J=1,2
      WRITE(3,103)Y(K),F(J)
  103 FORMAT(2X,'Y/D=',F5.2,3X,'FAN=',F4.1)
      WRITE(3,100)
      DO I=1,22
      UP(K,J,I)=(1.414*ESV(K,J,I))/((1.-(VO/V(K,J,I)**2.)*V(K,
     $J,I))
      VP(K,J,I)=(1.414*EDV(K,J,I))/((1.-(VO/V(K,J,I)**2.)*V(K,
     $J,I))
      WP(K,J,I)=(1.414*EDWV(K,J,I))/((1.-(VO/V(K,J,I)**2.)*V(K
     $,J,I))
C
C      S=SENSITIVITY
C
      S(K,J,I)=(1.-(VO/V(K,J,I))**2.)*V(K,J,I)/1.414
      UPVP(K,J,I)=(RABV(K,J,I)*GAV(K,J,I)*GBV(K,J,I))/(4.*(S(K
     $,J,I)**2.))
      UPWP(K,J,I)=(RABW(K,J,I)*GAW(K,J,I)*GBW(K,J,I))/(4.*(S(K
     $,J,I)**2.))
    2 CONTINUE
      WRITE(3,101)(X(I),UP(K,J,I),VP(K,J,I),WP(K,J,I),UPVP(K,J
     $,I),UPWP(K,J,I),I=1,22)
  100 FORMAT(5X,'X',8X,'UZ/UO',12X,'UR/UO',12X,'UD/UO',12X,'UZ
     $UD/UO',12X,'UZUR/UO')
  101 FORMAT(3X,F4.1,5X,F9.5,11X,F9.5,11X,F9.5,11X,F11.7,11X,F
     $11.7)
      WRITE(3,102)
  102 FORMAT(///)
    4 CONTINUE
      STOP
      END

/DATA
```